CR-137682
AVAILABLE TO THE PUBLIC

NA-75-227

TESTING OF LIFT/CRUISE FAN EXHAUST DEFLECTOR

By Donald W. Schlundt

March 1975

Prepared under Contract NAS 2-7657 by
ROCKWELL INTERNATIONAL
Los Angeles, California

for

AMES RESEARCH CENTER

NATIONAL AERONAUTICS AND SPACE ADMINISTRATION

CONTENTS

SUMMARY

A lift/cruise exhaust deflector system for the LF336/A tip turbine lift fan was designed, built, and tested to determine the design and performance characteristics of a large-scale, single swivel nozzle thrust vectoring system. The exhaust deflector static testing was performed at the Ames Research Center outside static test stand facilities. The test hardware was installed on a hydraulic lift platform to permit both in and out of ground effect testing. The exhaust flow of the LF336/A lift fan was vectored from 0° through 130° during selected fan speeds to obtain performance at different operating conditions. The system was operated with and without flow vanes installed in the small radius bends to evaluate the system performance based on a proposed method of improving the internal flow losses. The program also included testing at different ground heights, to the nozzle exhaust plane, to obtain ground effect data and the testing of two methods of thrust spoiling using a duct bypass door system and nozzle flap system.

The method of rotating the swivel nozzle to provide thrust vectoring proved to be a successful concept, however, the performance characteristics obtained during thrust vectoring were not favorable. The force measurements taken during the zero-degree vectoring cruise position achieved a thrust loss of less than 3% at 90% fan speed with the incorporation of turning vanes, but a substantial decrease in performance was obtained in all tested configurations as the vectoring angle was increased. The configuration with flow vanes attained the highest thrust coefficient value operating in the 90° nozzle position of only .86 at 90% fan speed and the configuration without flow vanes obtained the lowest value of less than .80 operating in the 90° position at high fan speeds.

INTRODUCTION

The single swivel nozzle exhaust deflector was selected as a vectoring system to be further investigated and tested based on studies that indicated the system to be an advantageous method of thrust deflecting for V/STOL vehicles using low-pressure ratio propulsion systems. The system could potentially be designed to be simple, low risk, lightweight, aerodynamically beneficial when integrated with a vehicle design, and considered to have accoustical advantages. Performance characteristics of a single swivel nozzle designed for a low-pressure ratio propulsion system were not available and large-scale model testing was proposed to establish valid installation criteria. The purpose of the static test program was to provide large-scale data on design and performance criteria of thrust vectoring forces, internal flow path conditions, system losses and thrust control methods for the

deflection concept.

The propulsion system designated for the test program was a J85-LF336/A tip turbine lift fan built by General Electric for previous test programs. The 91.5 centimeter (36-inch) diameter fan can provide a fan pressure ratio of 1.3 at the maximum performance rating. The deflector test hardware built for the LF336/A fan system was designed to represent a typical aircraft installation for aerodynamic considerations and also designed with minimum complexity to allow for manufacture and assembly without high cost or difficulty. The diffuser and nozzle sections were designed for simple modular welded construction, with special attention given to the bearing design to provide a swivel system that would represent a simple, but realistic, method of rotating the nozzle. The single swivel nozzle design consists of an exhaust nozzle attached to an S-curved duct with a double ring thrust bearing located in the bend of the duct. Rotation of the bearing directs the nozzle to the desired position through an arc from 0° through 130° controlled remotely through a chain link driven by a geared motor.

SYMBOLS

A_B bypass door open area, cm^2

A_D duct cross-section area, cm^2

A_E nozzle exhaust cross-section area, cm^2

C_T total thrust coefficient, $\frac{\text{total thrust vector}}{\text{calibrated total thrust}}$

F_H horizontal thrust vector, newtons

F_{Vo} vertical thrust vector, newtons

F_V vertical vector (with no spoiling), newtons

F_{VMAX} maximum vertical thrust vector, newtons

F_s side thrust vector, newtons

F_t total thrust vector, newtons

M_D diffuser exit mach number

N_F fan speed, rpm

P_o measured ambient pressure, newtons/cm^2

P_{SB} static pressure at small radius bends, newtons/cm^2

P_{SD} diffuser exit static pressure, newtons/cm^2

P_{TD} diffuser exit total pressure, newtons/cm^2

P_{TN} exhaust nozzle total pressure, newtons/cm^2

T_{TD} diffuser exit total temperature, °K

T_{TIN} fan inlet total temperature, °K

T_W outside wall temperature, °K

W_T total exhaust gas flow, kg/sec

β_b angle of bypass door thrust spoiler, deg.

β_f angle of nozzle flap thrust spoiler referenced to the nozzle (exit) axis, deg.

δ_o relative absolute pressure ratio

$$\frac{\text{measured ambient pressure}}{\text{standard pressure}}$$

θ_o relative absolute temperature ratio

$$\frac{\text{measured ambient temperature}}{\text{standard pressure}}$$

ψ angle of rotation of the swivel nozzle at the bearing, exhaust nozzle aft = 0°, deg.

Newtons = 4.4482 x pounds force

Kilograms = .4536 x pounds weight

Centimeters = 2.54 x inches

°Kelvin = 5/9 x °Rankine

TEST FACILITY

Test Stand

The lift/cruise fan exhaust deflector test was conducted on the outside static test stand at the Ames Research Center, Moffett Field, California. The static test stand is a concrete pit 15.2 by 18.3 meters, 1.83 meters deep (50 by 60 feet, 5 feet deep), covered by grating. The grating is heavy bridge decking over support beams capable of supporting loads of 48,700 kilograms per square meter (10,000 pounds per square feet). A "T" shaped center section of the deck is mounted on a 6800 kilogram (15,000 pound) capacity hydraulic lift, capable of vertical translation up to 3.05 meters (10 feet) above the fixed pit grating. This 3.05 meters plus the 1.52 meters to the pit floor (10 feet plus the 5 feet) is sufficient to elevate most test articles above the ground effects. The hydraulic lift can be translated up or down to obtain ground effects and by covering the grating with steel plating (as performed for the test program) the ground height of platform can be reduced to nearly zero if desired. The test stand can, therefore, permit both in and out of ground effect testing. The three extentions forming the "T," which is the working platform, measure approximately 1.52 by 2.44 meters (5 by 8 feet) each. The platform in the raised position can be rotated, but wind and test parameter rotational moments were restrained by cable stops.

Control and Data Acquisition

A control room for operation of J85 gas generator and LF336/A fan system, remotely controllable test model components and all data acquisition equipment was located adjacent to the test stand. An instrument panel containing calibrated gauges and controls was used to moritor the propulsion condition, nozzle position, and thrust spoiler device position.

The basic functions of the data acquisition system, including signal conditioning (amplifier, filter, etc.), integrating digital voltmeter measurements (analog to digital converter) and recording were accomplished by a Vidar Data Acquisition System and Teletype Paper-Tape Punch and Repco Printer. The system accepts 90 low-and-high-level DC inputs and 10 low frequencies. The scanivalve control and conditioning unit provides conditioning for up to 12 scanivalve modules.

The data recorded on tape from the Vidar Data Acquisition System was run through a data reduction computer program where the test data input signals are converted to measurement parameters. The test data print-outs and list-

ings of forces, pressures, temperatures, and speeds were investigated and corrected for computer program variations and load cell values during testing period to establish data validity. All data print-outs and listings were in the customary U. S. units of measurement and were converted, where necessary, to International System of Units for the report.

MODEL AND APPARATUS

Propulsion System

The propulsion system used for the deflector test program was the LF336/A lift fan system designed and built by General Electric Company for NASA under contract number NAS 2-4130. The LF336/A fan is a single-stage, tip-turbine, rotor-stator design with a maximum pressure ratio of 1.3 and a fan diameter of 91.5 centimeters (36 inches). One J85-5 turbojet engine is used to supply the driving gas to the tip-turbine blades of the fan through a ducting arrangement that distributes the flow equally to each half of the 360° scroll. A design fan to turbine flow bypass ratio of approximately 5:1 provides a total exhaust flow of 119 kilograms/second (262 pounds/second) at the maximum design rating of 24600 Newtons (5550 pounds) operating at a fan speed of 6047 RPM. The fan was mounted in the test stand with its axis in a horizontal plane as shown in figures 1 to 7.

Model

The deflector system hardware was designed for direct use with available LF336/A lift fan hardware with an objective of minimum complexity to allow for low-cost fabrication. As shown in the test hardware schematic, figure 8, the system consists of diffuser and nozzle sections with a bearing between the two sections to allow the nozzle to rotate.

The exhaust diffuser section was designed to provide low-expansion losses of the fan and tip-turbine discharge flow from the fan exit plane to the maximum duct area used through the bend. A 76.2 centimeter (30 inch) exhaust hub cone of an ellipse design, used with the LF336/A lift fan for previous tests at NASA/Ames, was combined with 5° diffuser duct angle to provide an effective exhaust expansion half-angle of 10.5°. The circular duct section through the bend was sized to provide a flow velocity of less than .3 mach number to minimize internal flow losses.

The change in duct flow area from the maximum area through the bends to the designed minimum nozzle area was based on a constant straight-line area

reduction from the circular swivel bearing to the oval shape at the nozzle exhaust plane. The nozzle section shape was formed by maintaining a constant maximum dimension of the bearing in the top and bottom walls while in the side walls the dimensions were reduced by a half-angle of approximately 10.5 degrees at the extreme of each side to obtain the minimum area at the exhaust plane. The nozzle shape was selected to represent a typical aircraft installation for providing a low aerodynamic drag design.

The deflector system test hardware was designed to allow for simple, low-cost fabrication by modular construction that was made in partial sections then assembled by welding and machining the sections to form the complete deflector system.

A method of rotating the nozzle by a bearing offered an appreciable advantage for the test program over a fixed bolted flange attachment that would require physical effort and time to position the nozzle for different deflection angles. A system using two overlapping rings was found to be not only the most promising method for the test application, but also a type of bearing that would be considered for aircraft design. The test program proved the bearing was simple, low cost, reliable and met the performance objectives. A Haynes Stellite alloy was initially selected as the bearing material with the most favorable properties, but due to the higher cost of obtaining and machining large Stellite rings a 17-4 steel alloy was chosen as the material for the test hardware. A dry lubricant "Vitrolube 1220" that can provide good lubrication during high-temperature operation was applied to the contact surfaces of the rings to reduce the coefficient of friction during bearing rotation. The method of turning the swivel to the desired nozzle position was done with a chain link around the outside bearing flange, driven by a geared electric motor scheduled to rotate the bearing approximately 20° per second. The operation of the motor in either direction was performed remotely in the control room during the test.

The test program included the use of flow guide vanes or splitters to obtain information on a method of minimizing internal turning losses through the bends. Two sets of vanes were made from .292 centimeter (.125 inch) thick steel plate machined on each edge. The turning vanes, as shown in the test hardware schematic in figure 8, were installed in the 65° angle small radius bends of the diffuser duct section prior to the bearing plane and aft of the bearing plane in the nozzle section. The vanes extend throughout the length of the bend and width of the duct and divide the flow path by using a constant radius-to-width ratio. A third vane located on the duct bend centerline was considered as part of both the diffuser and nozzle vane design, but due to the size and weight of the larger vane hardware, a decision was made to not use large vanes in this test program.

Two methods of lift/cruise fan thrust spoiling were selected to be included as part of the exhaust deflector program. The bypass door thrust spoiler, shown in the test hardware schematic in figure 8, was a 38 x 24 centimeter (15 x 9.5 inch) size hinged door installed in a frame to simulate an aircraft nacelle installation and located on the top portion of the diffuser section. The nozzle flap thrust spoiler was a .12 thickness to chord length ratio airfoil installed across the center of the narrow horizontal axis of the oval nozzle. The airfoil was 42.1 centimeters (16.6 inches) long, as shown in figure 45, with the split portion 27.4 centimeters (10.8 inches) long installed with the hinges on the nozzle exit plane. As the two parts of the hinged flap were split at increasing angles to the nozzle flow direction axis, the split flap formed a higher angle wedge in the nozzle exhaust stream. Both the bypass door and nozzle flap thrust spoiler systems were actuated with electric motors that were remotely operated from the control room during the test.

The LF336/A lift fan, J85 gas generator and deflector system test hardware were mounted in a supporting frame, as shown in figures 1 through 7. An existing frame that had been used for previous LF336/A fan testing was modified to allow for the deflector system installation and clearance for rotation of the swivel nozzle section. The deflector system was mounted to the frame to simulate an actual aircraft installation by a cantilever design linking the diffuser duct section to the frame. Three main links were used for thrust loads and three support links were used to take lateral and turning loads. There was no attachment between the fan frame and the deflector system other than a leaf spring seal to prevent any leakage of the fan exhaust flow. This fan frame and deflector separation was specified to prevent any possible damage to the fan system due to loads from the deflector system hardware during the tests. All loads from the deflector system were transmitted to the supporting frame. Three load cells mounted in clevis brackets between the supporting frame and the hydraulic lift platform, as seen in figures 1 through 7, were used to measure thrust forces.

Instrumentation

The total thrust forces produced by the LF336/A fan propulsion system with the exhaust deflector installation are measured by three strain gage load cells. Each of the three component load cells were mounted between the supporting frame and the hydraulic lift platform to measure the horizontal, vertical, and side vector forces. The load cells were calibrated in the laboratory and checked with the data acquisition system after installation on the test stand.

In addition to the ambient barometric air pressure and J85 turbine discharge pressure, 79 diffuser and nozzle section pressures were recorded for each data point. The diffuser exit rake was located approximately 80 centimeters (31.5 inches) downstream of the lift fan exhaust plane prior to the duct bend in the maximum duct diameter of 119.4 centimeters (47 inches). The diffuser exit rake, shwon in figure 9, contained 24 total pressure and 12 static pressure tubes located on the rake to provide an area weighted profile. The nozzle exhaust rake, shown in figure 10, was located at the nozzle exit plane. The nozzle rake contained 24 total pressure tubes also located to provide an area weighted profile. The diffuser section bend prior to the bearing, and nozzle section bend aft, of the bearing each contained 5 static pressure taps installed on the inside wall of the small radius bends, as shown in figure 11. the fan exhaust hub cone contained 9 static pressure taps equally spaced along the 76.2 centimeter (30 inch) length of the ellipse shape.

In addition to the ambient air temperature and J85 exhaust gas temperature, 25 fan inlet, diffuser and wall temperatures were recorded for each data point. The diffuser exit rake, shown in figure 9, contained 10 total temperature tubes located across the near horizontal bar of the rake to provide an area weighted profile except for the void of two tubes in the center portion. The 13 wall temperature thermocouples, shown in figure 35, were located on the outside skin of the diffuser, bearing, and nozzle sections. The 2 fan inlet thermocouples were located on the fan inlet strut. Prior to the ground effects and thrust spoiling system testing, there were 2 additional thermocouples installed in the fan inlet At that time, all 4 inlet thermocouples were removed from the data acquisition system and recorded on a Honeywell oscillograph.

The position of swivel nozzle, the angle of the bypass door thrust spoiler and the angle of the nozzle flap thrust spoiler were calibrated with guages on the instrument control panel in the control room. The J85 gas generator control throttle with a panel containing the engine RPM and turbine exhaust conditions were located on the operators section of the control panel. The fan speed was recorded by the data acquisition system and also provided for control room monitoring on a digital RPM display. Thermocouples measuring the fan bearing temperature were periodically checked with a bridge type indicator for monitoring the fan bearing condition.

TESTING AND PROCEDURE

The purpose of the fan exhaust deflector static test program was to provide large-scale data on design and performance criteria of thrust vectoring forces, internal flow path conditions, system losses, and thrust control methods for the deflection concept. Testing the test hardware on the hydraulic lift platform allowed for minimum ground effects during the test operation by providing high ground clearance, while in-ground effects were obtained by reducing ground clearance heights. Operating the deflector system during different fan speeds at selected exhaust deflection angles, from an aft zero-degree direction used for cruise through a 40° forward of vertical direction (130° deflection angle) used for the V/STOL mode, provided data that can be analyzed to establish a range of performance criteria.

A pretest report (NA-73-788) was prepared prior to the testing to define and outline the test program procedure. Along with a description of the facility, test hardware and required instrumentation, a complete test schedule was presented in the report. Part I of the schedule was to determine which of the deflector system configurations, operating with and without flow vanes installed in the small radius bends, would provide the best performance. The test hardware as described in the model design section, not including the flow vanes or the nozzle flap, thrust spoiler installed, was considered as the basic configuration. The diffuser bypass door, which is permanent hardware on the top of the diffuser duct wall, remained closed during the configuration performance testing. The four configurations tested in part I included the basic configuration, the basic configuration with vanes in the diffuser section bend, the basic configuration with vanes in the nozzle bend and the basic configuration in both the diffuser and nozzle bends. Three propulsion power settings selected as fan speeds of 90% (5400 RPM), 80% (4800 RPM) and 60% (3600 RPM) were run for each nozzle position. High fan speeds were considered a risk due to the fan hardware condition, therefore, only fan operation below 5400 RPM was specified for this program to prevent any possible damage to the fan system. The five nozzle positions selected for part I, as measured from the direct aft zero-degree direction, were 0°, 30°, 60°, 90°, and 130°. The ground clearance height for the performance tests was selected to allow for minimum ground effects by raising the hydraulic lift platform to the maximum allowable height of the lift system. The ground height was set at 3.05 meters (10 feet) from the exhaust nozzle plane in the 90° nozzle position to the pit grating, which provided a total height of 4.57 meters (15 feet) to the pit floor.

From the test results of part I, the configuration that produced the best performance would be used to complete the tests in the second part of the test program. Part II of the schedule included ground effects tests and the testing of two methods of thrust spoiling using a duct bypass door system

and a nozzle flap system. The test schedule in the pretest report had listed a number of different nozzle positions for each 90%, 80%, and 60% fan speed selected for these tests. Prior to the testing, the part II schedule was revised to reduce the number of test data points and testing time by performing all the runs with the nozzle in the 90° vertical thrust position.

The ground effect tests were run at ground heights of 305 centimeters (120 inches), 152 centimeters (60 inches), and 116 centimeters (45.75 inches). The bypass door thrust spoiler test was run at door angles of 0°, 20°, 50°, and 80° measured from the closed-door position as zero degrees. The nozzle flap thrust spoiler was run with the two parts of the hinged flap opened at angles of 0°, 15°, 30°, and 45° measured from the airfoil-shaped flap in the closed position as zero degrees. To minimize wind velocity effects, the outside static testing was run when wind velocities were less than 8 kilometers per hour (5 miles per hour). The fan speed was adjusted by the gas generator throttle to be as close as possible to the selected RPM before the data was recorded. The fan speeds were recorded up to 27 times for each data point and averaged to obtain a value for the condition.

The two recorded fan inlet temperature measurements for each run were averaged to obtain the absolute temperature ratio for that condition. Fan inlet temperatures were near outside ambient air temperatures when the deflector system was operating in the zero-degree cruise position, but temperatures measured during operation at high deflection angles were consistently higher than outside ambient. The increase in fan inlet temperature as the nozzle was rotated down indicates that exhaust flow circulation in the test stand area was partially ingested in the fan.

RESULTS

Configuration Performance Testing

The four configurations with and without flow vanes were tested as outlined in the test program procedure. When the system was operating at selected power settings in the zero-degree nozzle position the fan speed was fairly stable with little variation in RPM. As the vectoring angle was increased by nozzle rotation the fan speed became unsteady. At high deflection angles the fan speed fluctuated as much as ± 2 percent. The rapid fluctuation in fan RPM at high angles of deflection did not cause any problems during the testing and showed no effect on the test hardware.

The basic configuration without flow vanes was tested at nozzle angles of 0°, 30°, 60°, 90°, and 130°. In the 130° nozzle position the exhaust flow appeared to be impinging on the corner of the supporting frame and hydraulic lift platform. The concern of not obtaining valid performance at 130° deflection due to possible interference of the exhaust flow caused the change in the procedure for the remainder of the testing and test data was recorded at 110° rather than the 130° nozzle position.

The test data was normalized for the analysis and presentation to relate the environmental effects of the ambient temperature and pressure conditions measured during the testing. The recorded force measurements were corrected by the relative absolute pressure ratio to adjust the thrust values for the effect of ambient pressure. The recorded fan speed for each run was corrected by the absolute temperature ratio to adjust for the effect of the fan inlet temperature. The two recorded fan inlet temperature measurements for each run were averaged to obtain the absolute temperature ratio for that condition. Fan inlet temperatures were near outside ambient air temperatures when the deflector system was operating in the zero-degree cruise position, but temperatures measured during operation at high deflection angles were consistently higher than outside ambient. The increase in fan inlet temperature as the nozzle was rotated down indicates that exhaust flow circulation in the test stand area was partially ingested in the fan.

The force measurements were recorded in the horizontal, vertical, and side thrust vectors at selected fan speeds. Due to environmental effects and system control the propulsion system could not be regulated to operate exactly at selected constant fan speeds during the testing. When the recorded fan speeds were corrected for inlet temperatures the resulting values varied from the specified speeds. The test data was analyzed first as a function of corrected fan RPM before the parameters were obtained for constant fan speeds of 90%, 80%, and 60% RPM.

The horizontal forces, shown as deflector nozzle angle versus corrected thrust in figures 12, 13 and 14, illustrates the thrust change in the horizontal plane as the nozzle is vectored from 0° to 130°. The thrust change is nearly a function of the cosine of the turning angle, as might be predicted. The thrust value at 0° represents the maximum performance obtained at selected fan speeds in the horizontal direction. Except for the low fan speed condition, the configuration with all vanes installed obtained the highest performance in the horizontal plane. Thrust values not being zero in the horizontal plane while the nozzle position was at 90° indicates the exhaust flow had

turned slightly less than 90°. The configurations with all vanes and with nozzle vanes had better flow turning at high angles of deflection than the other configurations.

Figures 15, 16, and 17, which show the vertical corrected thrust versus deflector nozzle angle, illustrate the thrust change in the vertical plane as the nozzle is vectored from 0° to 130°. The thrust value at 90° represents the maximum performance obtained at selected fan speeds in the vertical direction. The thrust change from the 90° vertical nozzle position is nearly a function of the sine of the change in turning angle. The configuration with all vanes installed obtained the highest performance in the vertical plane than the other configurations, although, the vanes caused a higher vertical vector force in the 0° nozzle position that would not be desirable for horizontal thrust mode operation. A comparison of vertical to horizontal thrust data shows the vertical thrust at 90° to be less than the horizontal thrust at 0° for the same fan speed. This comparison indicates a decrease in performance as the nozzle is rotated from the 0° to 90° position.

The swivel bearing plane was placed 27.5° from vertical plane in the aft view and 27.5° from the exhaust centerline in the top-side view, as shown in the hardware schematic in figure 8. The exhaust flow path was designed to be directly horizontal in the 0° nozzle position and directly vertical in the 90° nozzle position. The nozzle rotation on the bearing plane causes the exhaust flow path to arc, which generates a side force. The side forces, shown as deflector nozzle angle versus corrected side thrust in figures 18, 19, and 20, illustrate the thrust change in the side plane as the nozzle is vectored from 0° to 130°. The side force is nearly a function of the sine of the angle of the nozzle centerline to the true 0° to 90° plane. The configurations with the nozzle vanes appear to have the least side force in the 0° and 90° nozzle positions, but show the highest side forces at other nozzle positions. A minimum side force in all nozzle positions is desirable, although, it is a trade of performance, design, and installation requirements. Since the nozzle vanes do improve the side force in the 0° cruise position, the configurations that include nozzle vanes would be better for side force design than the configurations without nozzle vanes.

The sum of the horizontal, vertical, and side vector forces was made to establish the total vector force for each test run. The corrected total thrust versus corrected fan speed for all four configurations is shown in figures 21 and 22 for 0°, 30°, 60°, and 90° nozzle positions. The figures illustrate that the configuration with both sets of flow vanes installed in the diffuser and nozzle small radius bends provided the highest performance in all nozzle positions when operating at high fan speeds.

A calibration of the LF336/A lift fan propulsion system on the test stand was proposed to obtain optimum performance of the system with a near ideal nozzle installation to use as a comparison for the deflector test performance. Due to the time and cost to assemble and run a calibration of the lift fan system with new exhaust nozzle hardware, the additional procedure was eliminated from the deflector program schedule. For the purpose of comparison, the data from the LF336/A lift fan test program (NAS2-4130 contract) was used to compare the performance of the lift fan system without a deflector system installed to the deflector test results. The lift fan test program was performed in 1968-1969 with the same gas generator and fan hardware used for the deflector system test, but equipped with a measuring section exhaust system installed for calibration. The LF336/A lift fan performance calibrated test data is shown in figure 23 as corrected thrust versus corrected fan speed.

The total thrust coefficients were calculated for deflector system test data, shown in figures 24, 25, and 26 as thrust coefficient versus deflector nozzle angle, to provide an estimate of the thrust loss caused by the exhaust deflector system as the nozzle was rotated from 0° through 130°. The total thrust coefficients (C_T) were obtained from a ratio of the total thrust vectors, presented in figures 21 and 22, divided by the calibrated total thrust for selected fan speeds of 90%, 80%, and 60%. All four configurations tested indicated the same trend of a substantial decrease in C_T as the deflector nozzle angle was increased. The data also shows a greater performance loss at lower fan speeds than high fan speeds for the same vectoring angle. The configuration with both diffuser and nozzle vanes installed provided the highest coefficient, at high fan speeds, of the configurations that were tested. The C_T value of .97 for the all-vane configuration operating in the zero-degree cruise position at 90% fan speed was the highest value obtained in the test, but an extrapolation of the test data indicates a C_T value higher than .97 would be achieved if the system were operating at fan speeds over 90%.

The configuration with both sets of vanes attained a C_T value of only .86 operating in the 90° nozzle position at 90% fan speed. Except for the low fan speed performance, the configurations without vanes or with only diffuser vanes obtained the lowest C_T values of less than .80 operating in the 90° position. An extrapolation of the all-vane configuration data would indicate higher performance at fan speeds over 90%, but C_T values of less than .90 might be expected.

The diffuser exit total and static pressure ratios versus tube location on the rake are shown in figures 27 and 28. The pressure distribution data is shown for the basic configuration without flow vanes installed that was recorded in 0° and 90° nozzle positions at 90%, 80%, and 60% fan speed. The

pressure profiles for the other configurations varied only slightly from the basic configuration and are not shown because of similarity.

The diffuser exit total pressures of the tubes near the duct wall are relatively lower than the tubes near the center and are also more constant for each fan speed out to about 40 centimeters (16 inches) from the wall. The tip turbine flow of the LF336/A, discharged near the wall, is designed for an exit total pressure of approximately 10% lower than the fan exhaust flow at the maximum static rating. The pressure pattern of the tubes on both sections of the cross-bar diffuser rake, shown schematically in figure 9, are very similar and clearly indicate the turbine lower pressure flow near the wall and fan exit flow in the center portion. The fan exit flow pressures of tubes 7, 8, 17, and 18 show a similar high and low recording at the same distance from the center for each fan speed. The turbine discharge pressures are consistently higher in the 90° nozzle position than in the 0° cruise position which is shown by the data recorded from the pressure tubes near the duct wall.

The diffuser exit static pressure ratios are fairly constant across the rake for each fan speed except for tubes 5 and 6 located near the duct wall. The static pressures in the 90° nozzle position are higher than in the 0° cruise position for each tube in all fan speeds.

The total and static pressure tubes on the diffuser rake were placed in an area weighted location. Values from the total number of tubes for the total and static pressures of each run were averaged for the 0° and 90° nozzle positions of all four deflector configurations. These average pressures were used to obtain the duct mach numbers, shown in figures 29 and 30, as a function of corrected fan speed for 0° and 90° nozzle positions. The mach number values ranged from approximately .26 to .19 for fan speeds of 90% to 60%. An extrapolation of the data would indicate the mach number to be about .30 at 100% fan speed which is only slightly higher than the mixed flow exhaust velocity used to size the duct design from LF336/A design data.

The mach numbers acquired from the test data analysis were used to obtain a weight flow/area function values. Using the design cross-sectional area of the duct, which was 11200 centimeters squared (1740 inches squared), corrected flow rates were calculated from these weight flow/area function values. The corrected total exhaust flow of the duct is shown in figures 31, 32, and 33 versus corrected fan speed for 0° and 90° nozzle positions. The corrected total exhaust flow value for the LF336/A design rating at 100% fan speed is about 120 kilograms/second (264 pounds/sec) and is close to the values obtained from extrapolating the data. The flow rates at high fan speeds for all configurations are higher for the 0° nozzle position than the 90° position. The corrected flow values for the two nozzle positions, shown in figure 33, versus nozzle angle, illustrate the trend of flow reduction as the flow was

deflected. The configuration with all flow vanes installed appears to have the least change in flow rate and the basic configuration without flow vanes has the highest flow rate change as the nozzle is rotated.

The diffuser exit rake also included total temperature tubes across one of the two cross-bars, as shown in the rake schematic of figure 9. The temperature tubes were located to provide an area weighted profile except for the void of two tubes in the center portion. The duct total temperature ratioed by the fan inlet temperature is shown in figure 34 versus tube location for the basic configuration without vanes in the 0° and 90° nozzle position. The other configurations tested with flow vanes installed provided similar temperature distribution. The higher temperature ratio of the tubes near the duct wall illustrates the high temperature of the turbine discharge and the center portion of the rake is low temperature fan exit flow. The temperatures at the rake, located approximately 80 centimeters (31.5 inches) downstream of the lift fan exhaust plane, indicate that fan and turbine exhaust flows are beginning to mix more near one wall than the other. The temperature ratios are higher in the 90° nozzle position than the 0° position for both the 90% and 60% fan speeds.

The outside wall temperatures of the deflector system were recorded during each run of the test program. The wall temperatures, shown in figure 35, are the maximum temperatures values obtained at the thermocouple locations during the testing when operating at 90% fan speed. The highest wall temperatures were at thermocouples located around the diffuser section and the lowest were near the nozzle exhaust area. The temperature pattern indicates that the hot turbine discharge is gradually mixing with the cooler fan exhaust as the gas flows through the system. The pattern also shows that the top part of the diffuser and nozzle sections are contacted by more of the cooler fan flow when the nozzle is either in the 0° cruise position or rotated to the 90° vertical position. System operation at higher fan speeds could increase the overall wall temperatures by approximately 30° Kelvin (54° Rankine) but longer periods of operation would have little change in wall temperatures since the values were fairly stable when recorded during the test program.

The diffuser section bend prior to the bearing and nozzle section aft of the bearing each contained five static pressure taps installed on the inside of the small radius bends, as shown in figure 11. The position of each pressure tap inside the modular segments of the bends was on an increasing bend angle to the flow path starting into the turn. The static to ambient pressure ratio versus the bend angle, is shown in figures 36, 37, and 38, for the diffuser and nozzle bends at 90%, 80%, and 60% fan speeds. The static pressure data shown were obtained from tests of the basic configuration without flow vanes and the configuration with all vanes installed opera-

ting in the 0° cruise and 90° vertical nozzle positions. The static pressures in the diffuser bend are fairly constant throughout during all fan speeds for both the 0° and 90° nozzle positions. The static pressures in the nozzle bend are all substantially lower than in the diffuser, and also show an undesirable decrease in pressure as the bend angle increases with a pressure recovery toward the completion of the bend to establish a static to ambient pressure ratio of 1.0 at the nozzle exit plane. The nozzle bend static pressure patterns indicate a possible flow separation due to the pressure reduction throughout the bend. The static pressures in both bends were higher for the 90° nozzle position than the 0° position for all fan speeds, except for tap number 6 which is the first tap of the nozzle bend inside the bearing. The configuration with both sets of flow vanes provided higher static pressures at every tap in both bends with a significant improvement shown in the nozzle bend pressures due to the installation of nozzle vanes. The distribution of total pressures across the nozzle exit is also an indication of an irregular flow pattern in the nozzle. A change in nozzle bend design may be required to correct the flow path in the system.

The total pressure rake in the nozzle exit plane contained 24 tubes, as shown in figure 10, located to provide an area weighted profile. (Tube number 18 near the center on the near horizontal cross-bar was not in operation during the testing). The nozzle exit total to ambient pressure ratio versus the tube location from center to wall is shown in figures 39, 40, and 41 for 90%, 80° and 60% fan speeds. The total pressure data shown were obtained from tests of the basic configuration without flow vanes and the configuration with all vanes installed operating in the 0° cruise and 90° vertical nozzle positions. The pattern of the pressure ratios appear more scattered for the higher fan speed than the lower. The pressures of the right side of the horizontal cross-bar tubes 21 through 24 (located downstream of the nozzle small radius bend at 0°) and of the bottom half of the vertical cross-bar tubes 7 through 12 indicate high values in the 0° nozzle position and low values in the 90° position, except for a pressure fall-off of tube 24 at 0° and 90% fan speed. The pressure pattern of the left-side of the horizontal cross-bar tubes 13 through 17 and of the top half of the vertical cross-bar tubes 1 through 6 indicate an opposite trend where the 0° nozzle position has the lower values and the 90° position has higher values. Some of the data from tubes 7 and 19 show a range of pressure ratios that are only slightly over 1.0, which could be due to improper functioning of the tube. The nozzle rake required repair several times during the test program and the pressure readings of all the tubes may have not been accurate.

The nozzle total pressures from all the tubes on the nozzle exit rake were averaged for each run and ratioed by the diffuser exit average total pressure for the same run. The exhaust nozzle to diffuser exit total

pressure ratio versus deflector nozzle angle is shown in figure 42 for all four configurations operating at 90% and 60% fan speeds. The nozzle to diffuser pressure ratios show a very high percentage of pressure recovery of the flow through the deflector system at all deflection angles. The highest pressure loss was less than 2.5% for the basic configuration without flow vanes at 90° to 130° nozzle positions. The relatively small number and distribution of the pressure tubes in the diffuser exit and nozzle rakes are not sufficient to establish a valid average or profile of the pressures for a complete internal flow analysis. The test data only provides an estimate of the flow conditions in the exhaust deflector system. The large decrease in performance obtained with the system as the vectoring angle was increased could indicate an increase in total pressure loss through the duct. The ratio of exhaust nozzle to diffuser exit total pressure, however, show pressure recoveries higher than 99% for configurations including nozzle vanes operating at all deflector nozzle angles. Based on the data acquired from the test system instrumentation, the reason for the high performance losses during thrust vectoring might not be due entirely to total pressure loss but may be caused by a reduction in fan flow rate and a possible reduction in nozzle coefficient.

Ground Effects and Thrust Spoiling Testing

Based on a preliminary analysis of the part I test results of the four deflector system configurations with and without flow vanes installed, the configuration with flow vanes in both the diffuser and nozzle small radius bends was selected to be used for tests in the second part of the test program. All the testing performed in part II for ground effects and thrust spoiling investigation was run with the deflector nozzle in the 90° vertical thrust position.

The ground effects tests were run at ground heights of 305 centimeters (120 inches), 152 centimeters (60 inches) and 116 centimeters (45.75 inches). The ground height was measured from the nozzle exit plane in the vertical 90° nozzle position. The vertical thrust values from the test data recorded at near selected fan speeds were analyzed as a function of corrected fan speed to obtain thrust values for constant fan speeds of 90%, 80%, and 60%. The fan inlet temperature data recorded on a Honeywell oscillograph during part II of the test program was lost in the postal system while in transmit between NASA/Ames and Rockwell International. Due to the loss of the fan inlet temperature data and lack of other temperature instrumentation near the fan inlet and gas generator inlet the actual temperatures of the air into the propulsion system was not available during the testing performed in part II. From observation of the data being recorded during the ground effect testing and the temperature data recorded during the testing completed in part I,

the fan inlet temperatures obtained during operation at 90° vertical nozzle positions were consistently higher than outside ambient. For the purpose of analyzing the ground effect thrust data a fan inlet temperature of 302° Kelvin (545° Rankine) was assumed to calculate the corrected fan speeds.

The vertical thrust values for corrected fan speed values of 90%, 80%, and 60% ratioed by the maximum vertical thrust value obtained in the 90° nozzle position is shown in figure 43 versus the ground height to the nozzle exhaust plane. The vertical thrust at ground heights above 152 centimeters (60 inches) at all fan speeds was not effected by ground height but the thrust values obtained at a height of 116 centimeters (45.75 inches) shows a thrust reduction due to ground effects. The low ground height data indicate the thrust loss of 10% at 60% fan speed is greater than the losses obtained at higher fan speeds. A comparison of the ground effects as a function of exhaust nozzle diameter, based on an effective nozzle diameter of 90 centimeters (35.5 inches), shows the thrust in the vertical nozzle position is reduced when operating less than 1.5 nozzle diameters from the ground.

The testing of two methods of thrust spoiling using a duct bypass door system and nozzle flap system were performed at the maximum ground height set at 4.57 meters (15 feet) from the exhaust nozzle plane in the 90° nozzle position to the pit floor to minimize ground effects. The amount of spoiling obtained with each system for a constant fan speed was approximately the same for all three selected fan speeds, except for slightly higher thrust reductions during the bypass door spoiler tests at 60% fan speed than at 80% and 90%.

The 38 x 24 centimeter (15 x 9.5 inch) hinged door of the diffuser bypass door thrust spoiling system was tested at door angles of 0°, 20°, 50°, and 80° measured from the closed-door position. The estimated bypass open area to exhaust nozzle area ratio versus bypass door angle is shown in figure 44, using a nozzle area of 6350 centimeters squared (990 inches squared). The amount of thrust change as a ratio of vertical thrust obtained with the bypass door open ratioed by thrust with the bypass door closed is shown in figure 44 versus bypass door angle. The bypass door system attained 10% thrust spoiling with a maximum bypass open area of 12% of the exhaust nozzle area. A comparison of thrust change with bypass area change with other bypass door angles indicate that the ratio of percent thrust change to percent of nozzle bypass area is close to 1.0 for the spoiling system size tested.

The nozzle flap thrust spoiler was a .12 ratio airfoil, as shown in figure 45, installed across the center of the narrow horizontal axis of the oval nozzle with the flap hinges on the nozzle exit plane. The double flap spoiler was run with the two parts of the hinged flap opened at angles of 0°,

15°, 30°, and 45° measured from the airfoil-shaped flap in the closed position as zero degrees. The amount of thrust change with the flap open ratioed by the thrust with the flap closed is shown in figure 45 versus flap angle. The 38% thrust spoiling attained by the double flap at the 45° position was partially caused by a reduction in fan blade loading. As the flap was opened to 45°, after operating at selected fan speeds for the 0°, 15°, and 30° flap positions, the fan speeds increased and required approximately 2.5% reduction in gas generator speed to lower the fan speed back to selected 90%, 80%, or 60% values. During the 45° flap setting the total and static pressures were also significantly lower than values obtained at lower angle flap settings. The condition indicates that the fan was tending to increase speed due to a decrease in effective exhaust area, which would reduce the load on the fan. The reduction in gas generator drive energy allows an adjustment to a selected fan speed at a lower fan pressure ratio. A flap setting of 45° or higher would require gas generator and fan control to maintain stable fan operation.

CONCLUSION

The purpose of the lift/cruise fan exhaust deflector test program was to determine the design and performance of a large-scale single swivel nozzle thrust vectoring system. The test system hardware design operated successfully during the test program to provide a reliable, simple and low-risk method of thrust vectoring through a range of 0° through 130° for low-pressure ratio propulsion systems. The designed method of rotating the swivel nozzle to the desired position, using a simple overlapping double ring bearing controlled remotely by a geared motor, demonstrated a concept that could be used on large, low pressure, slow-rotating hardware with much lower cost and higher reliability than large conventional-type bearings. The installation of the deflector hardware as the exhaust system for the LF336/A lift fan proposed no operational problems or hardware effects during the test.

The performance characteristics of the deflector system hardware during thrust vectoring did not provide efficient propulsion system performance to use V/STOL aircraft design criteria. The forces measured in the horizontal, vertical, and side planes, during exhaust flow deflection provided a valid pattern of thrust vectors for the selected fan speed, but the total thrust vector obtained from the summation of the three forces compared to the calibrated fan performance revealed the high thrust losses produced by the deflection system. The total thrust coefficients (C_T) obtained from a ratio of the total thrust vector divided by the fan calibrated thrust showed a loss in performance of only 3% to 5% in the zero-degree vectoring position but an unacceptably high thrust loss of 15% to 20% was obtained as the de-

flector nozzle angle was increased to the 90° vertical position during operation at high fan speeds.

The hot temperature from the turbine exhaust, over 800° Kelvin (1440° Rankine) at 100% fan speed, is discharged along with diffuser duct wall and was expected to cause high wall and bearing temperatures. The wall temperatures recorded during the test indicate there was some mixing occurring as the fan and turbine exhaust flows through the deflector system because of the decrease in duct wall temperatures from the diffuser to nozzle sections. The test data temperatures of the nozzle wall will presently allow lightweight metals or composites to be used for construction of the section. If the fan and turbine exhaust flows were totally mixed the total temperature would be less than 400° Kelvin (720° Rankine) at 100% fan speed. It would be highly recommended to consider using an exhaust flow mixer in the deflector design to reduce the weight of the system due to the importance of propulsion system total weight for V/STOL aircraft design.

The test data obtained from the deflector testing performed at NASA/Ames will be a primary tool for finding the hardware design problem areas. Further investigation is necessary to design the single swivel nozzle thrust vectoring system to provide efficient propulsion system performance to use for V/STOL aircraft design criteria.

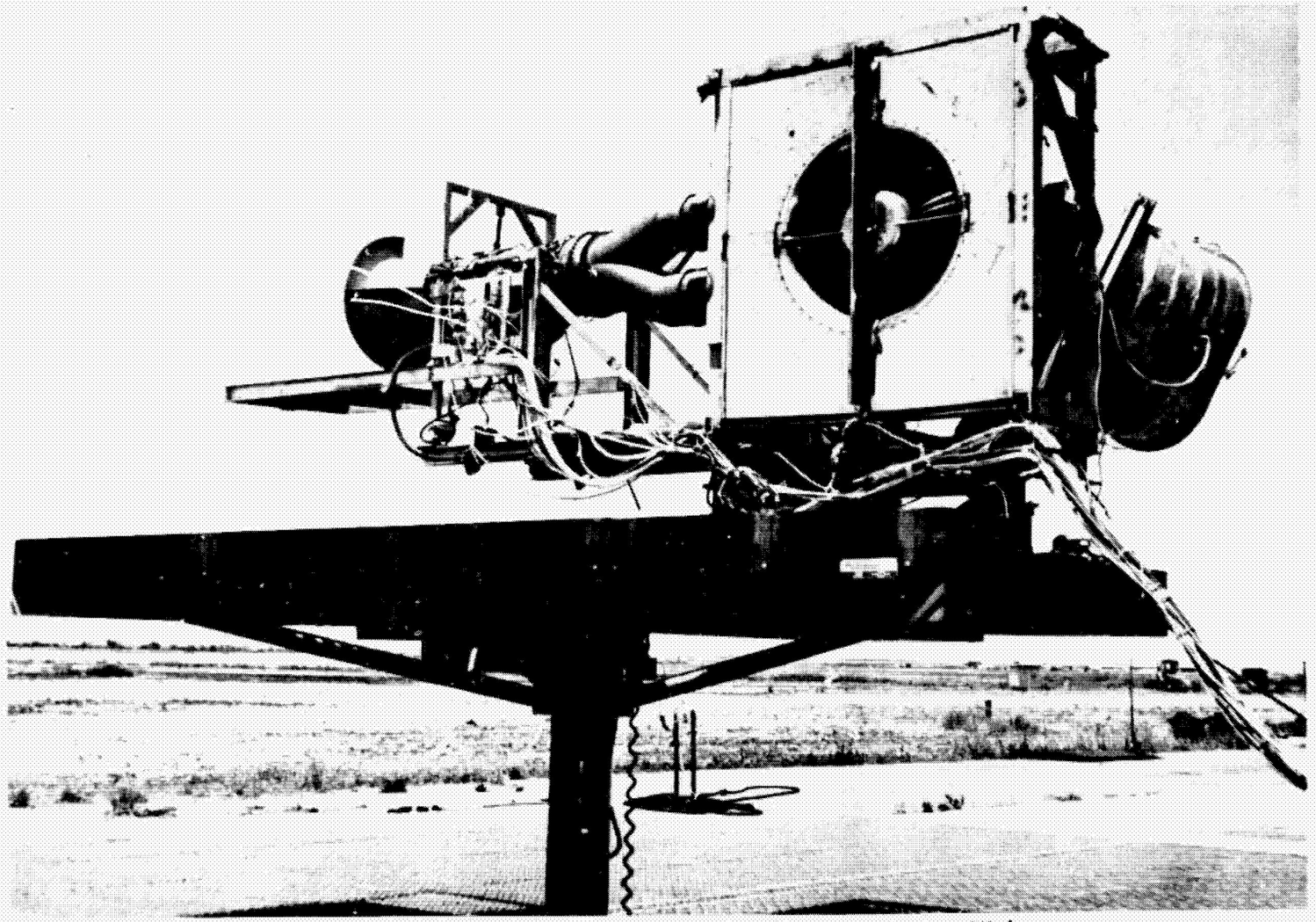

Figure 1. Front View of the LF336/A Lift Fan System With Exhaust Deflector Nozzle in 0° Cruise Position

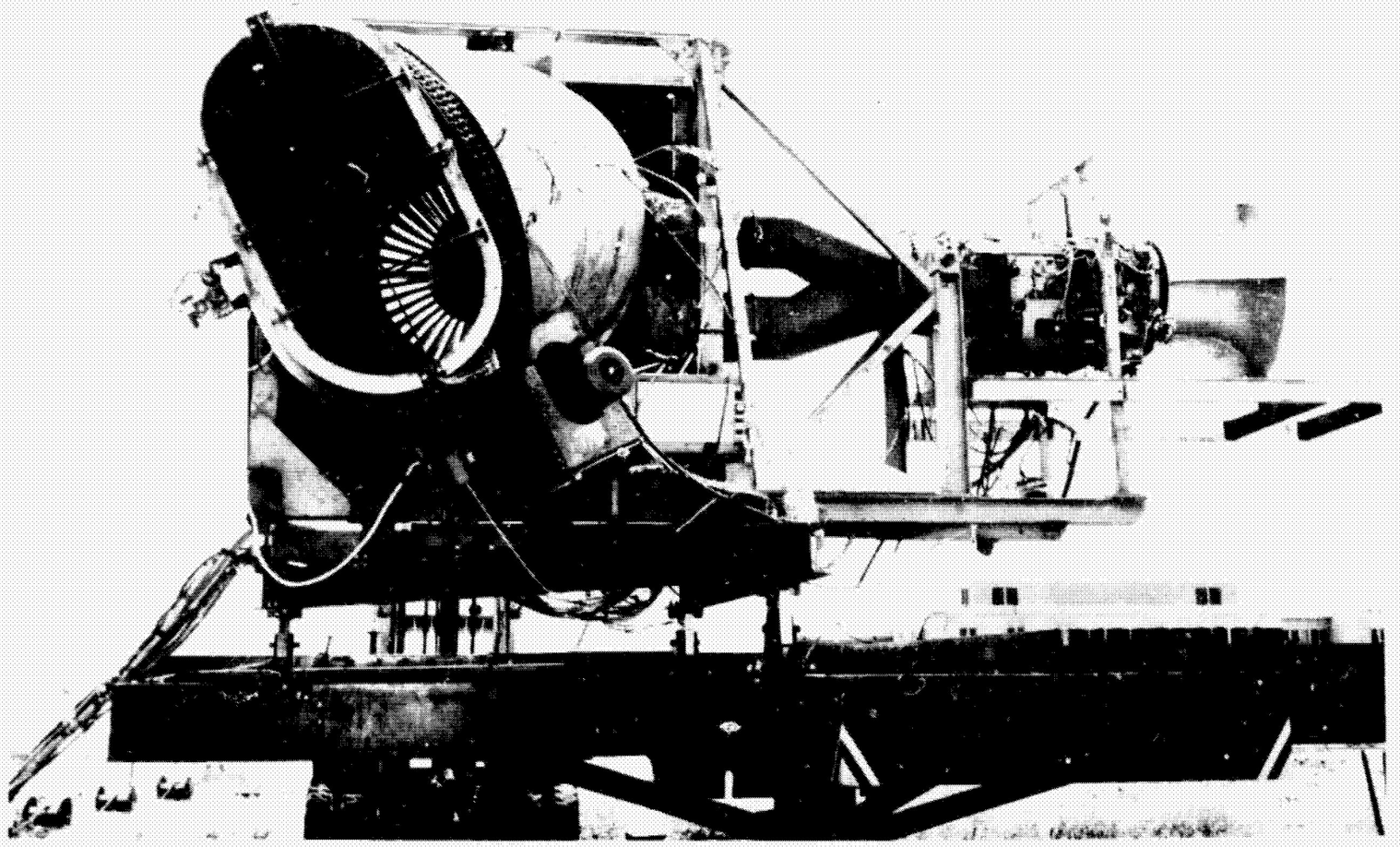

Figure 2. Aft View of Exhaust Deflector With Nozzle in 0° Cruise Position

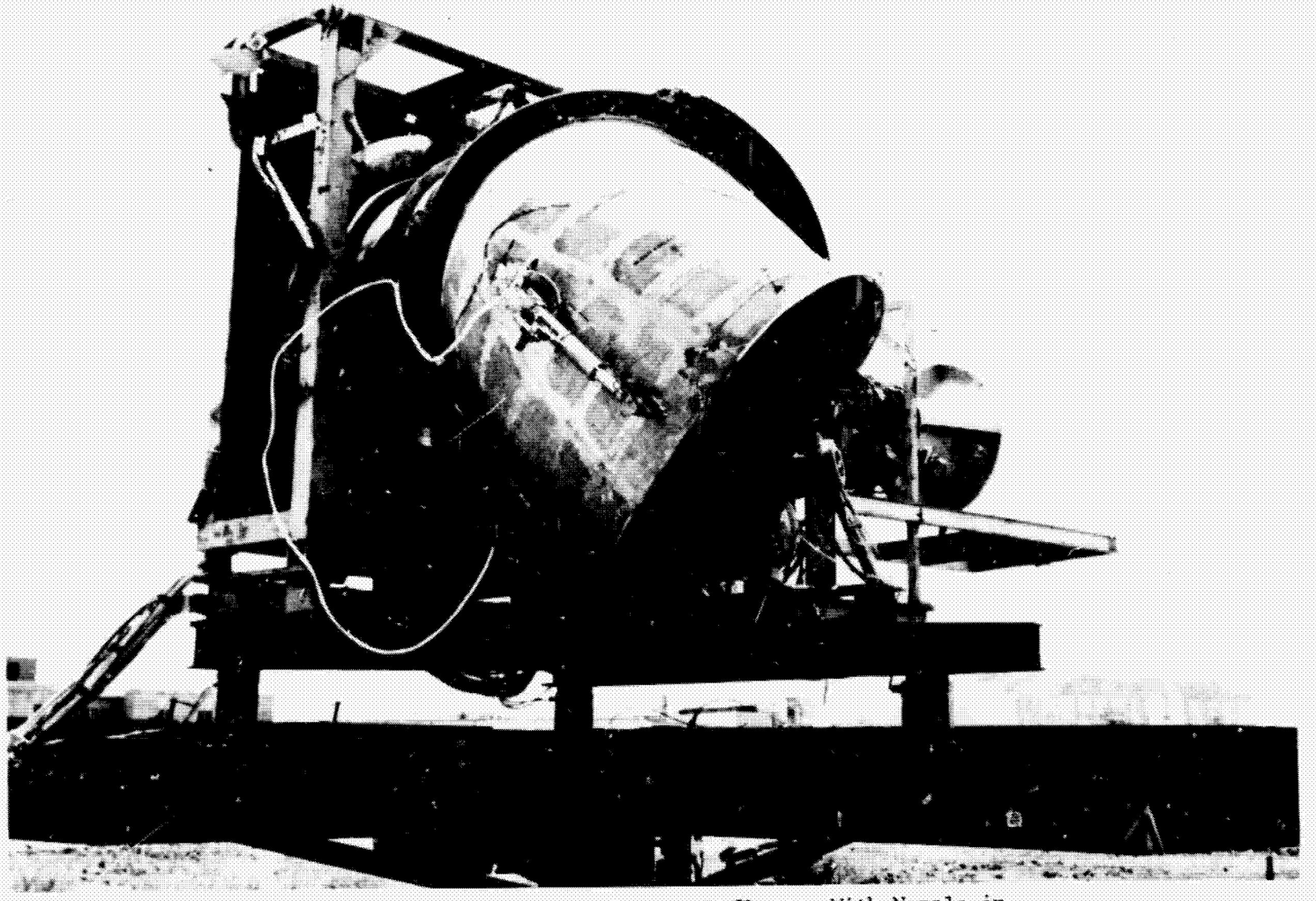

Figure 3. Side View of Exhaust Deflector With Nozzle in 60° Position

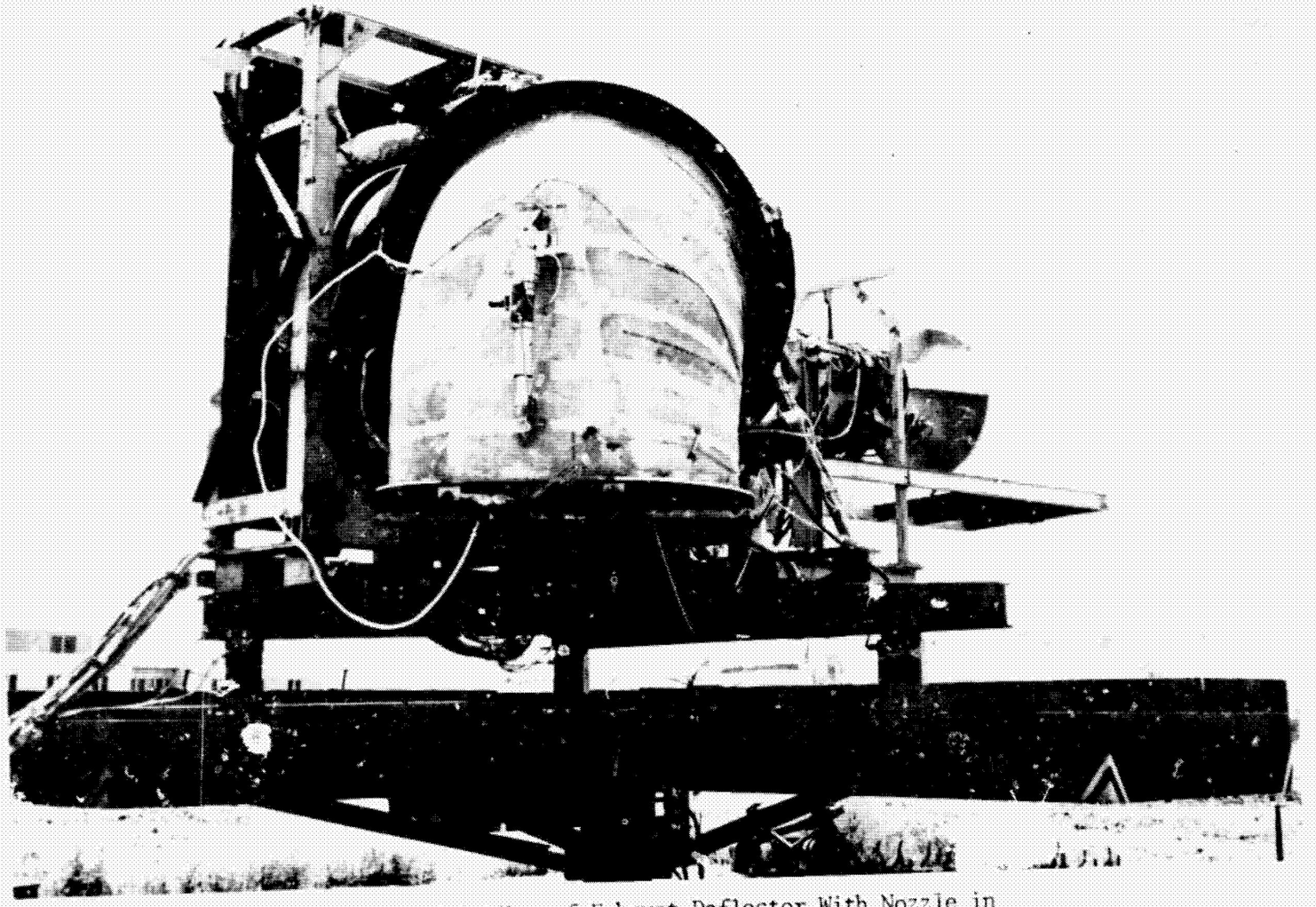

Figure 4. Side View of Exhaust Deflector With Nozzle in 90° Vertcial Position

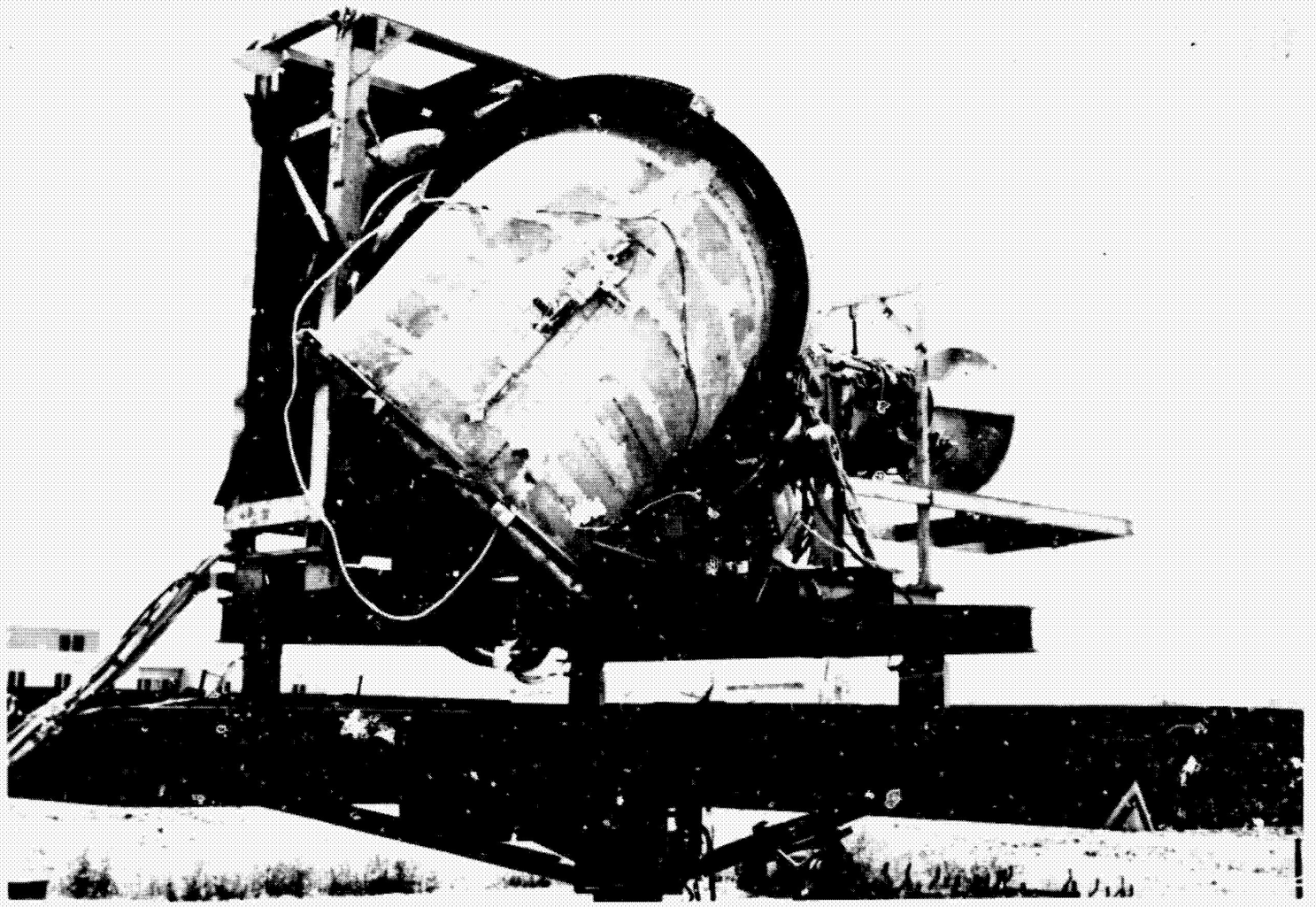

Figure 5. Side View of Exhaust Deflector With Nozzle in 150° Position

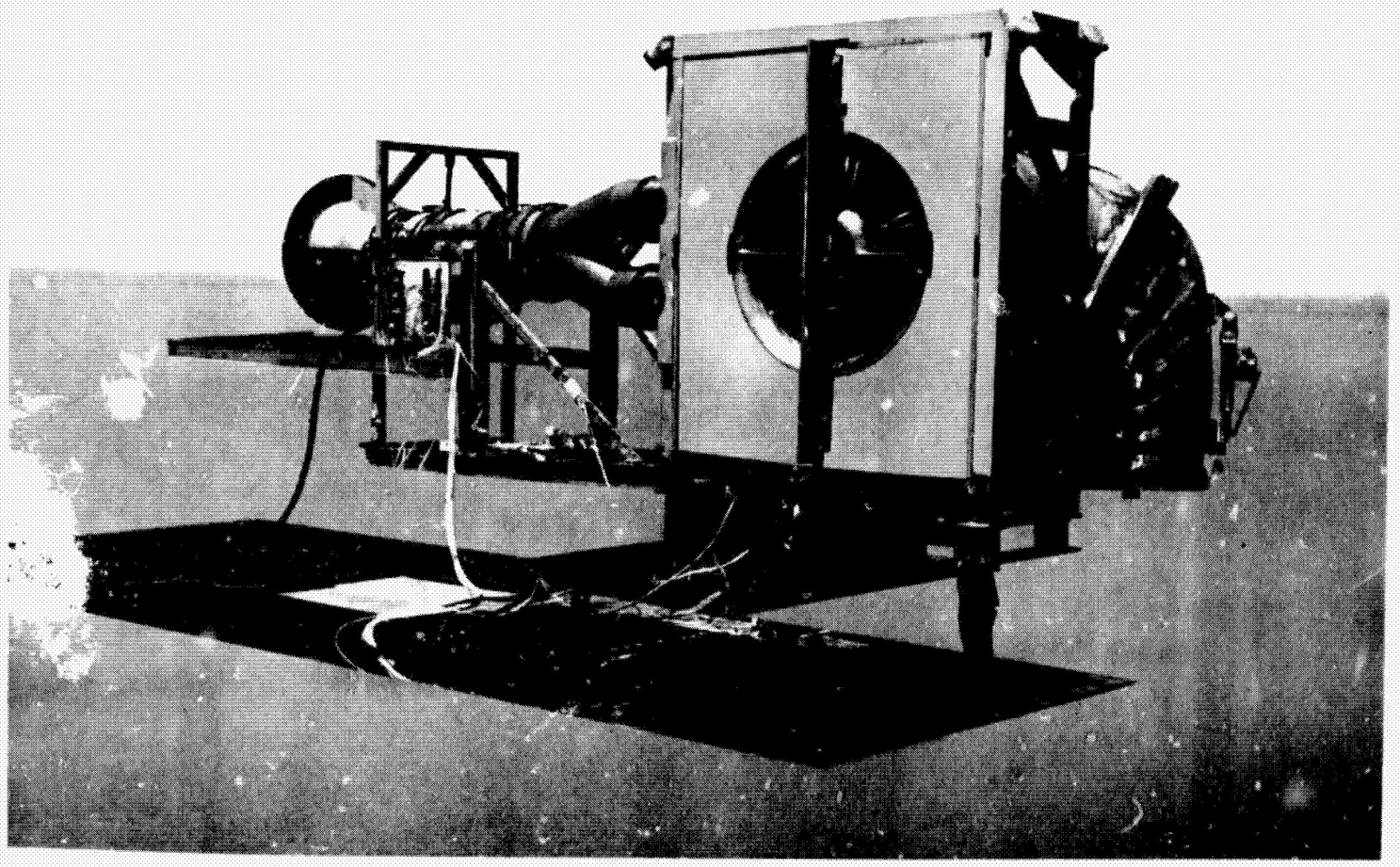

Figure 6. Front View of LF336/A Lift Fan System With Exhaust Deflector Nozzle in 90° Vertical Position

Figure 7. Aft View of LF336/A Lift Fan System With Exhaust Deflector Nozzle in 90° Vertical Position

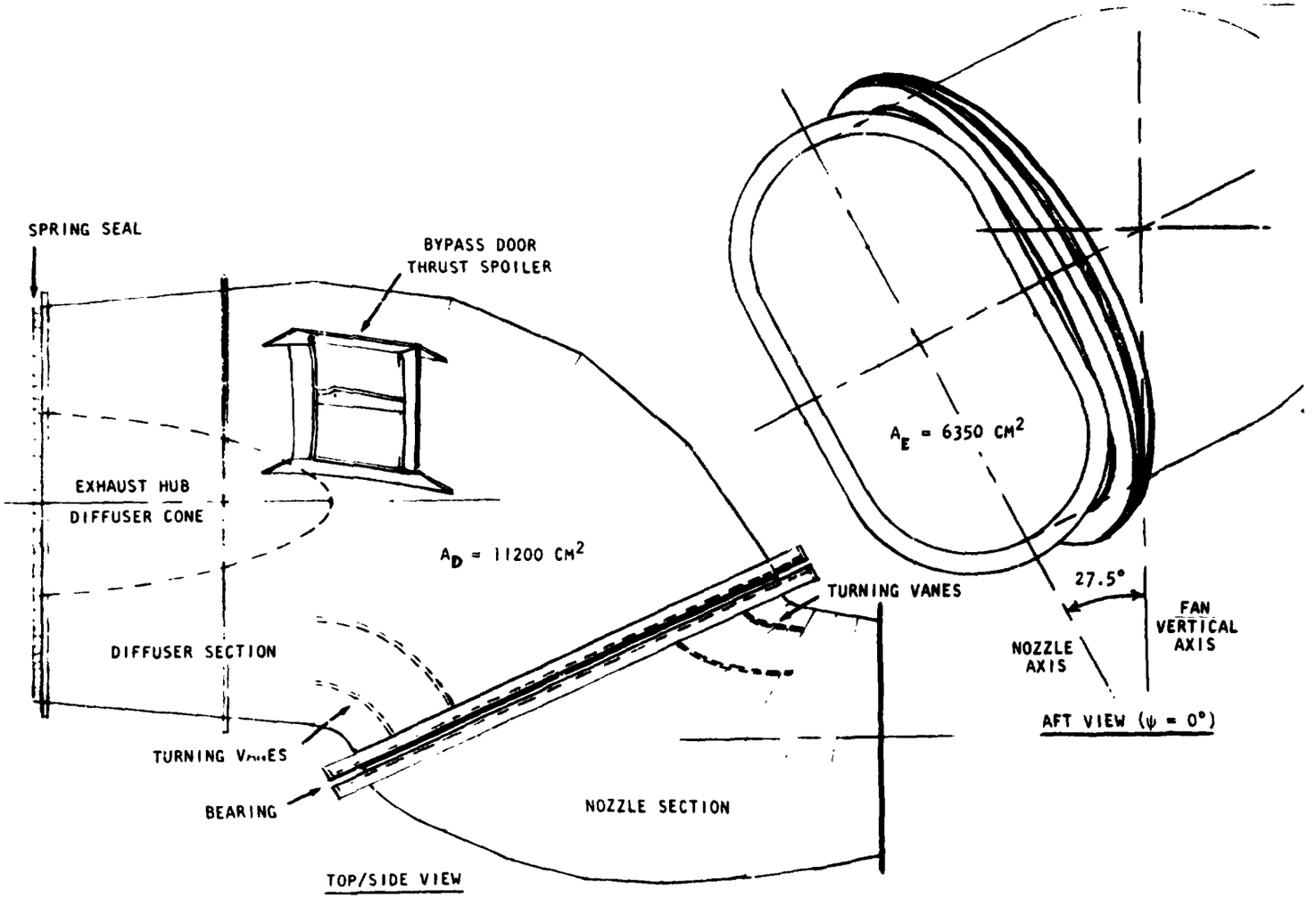

Figure 8. LF336/A Lift/Cruise Fan Exhaust Deflector System Test Hardware Schematic

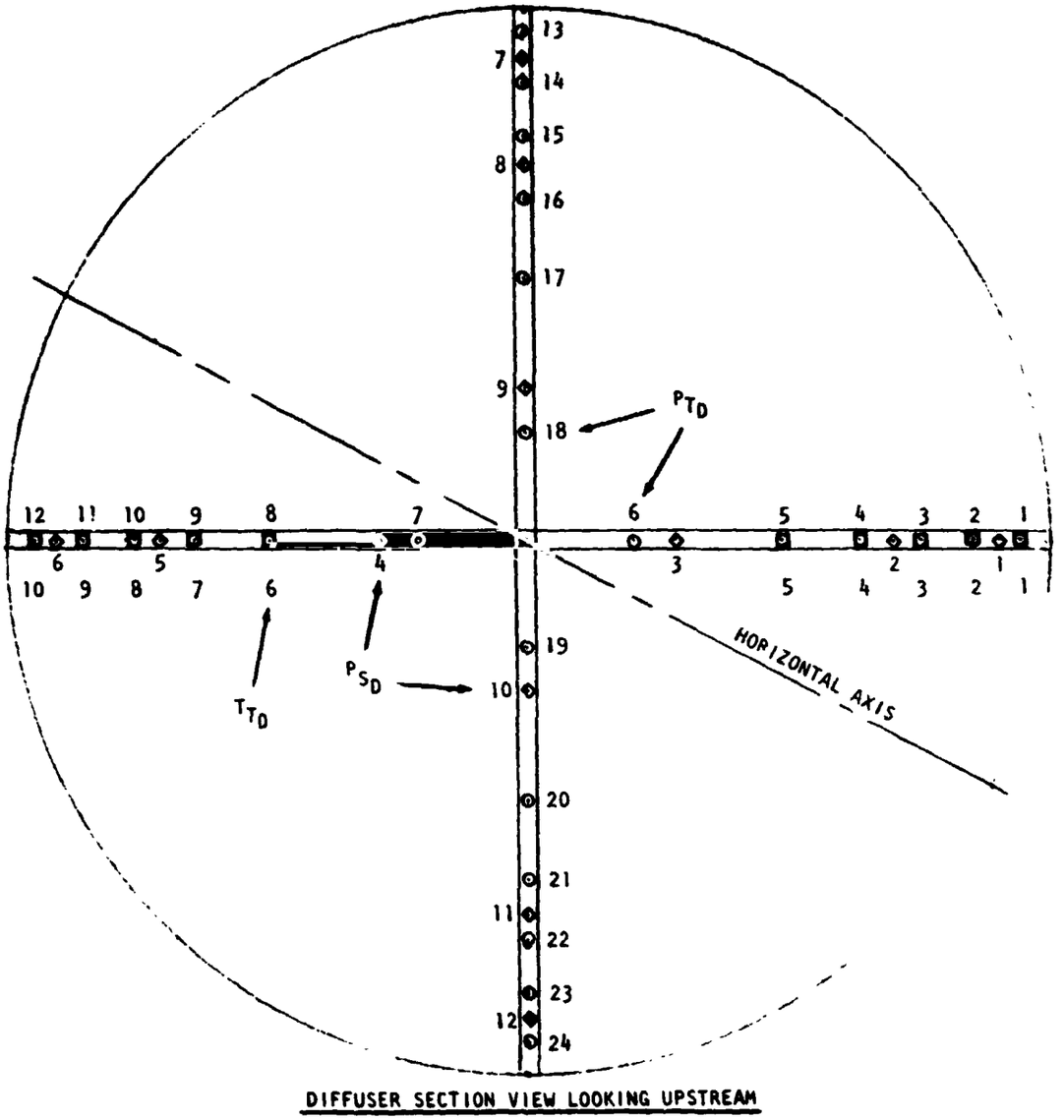

DIFFUSER SECTION VIEW LOOKING UPSTREAM

Figure 9. Diffuser Rake For Total Pressure, Total Temperatures, And Static Pressures

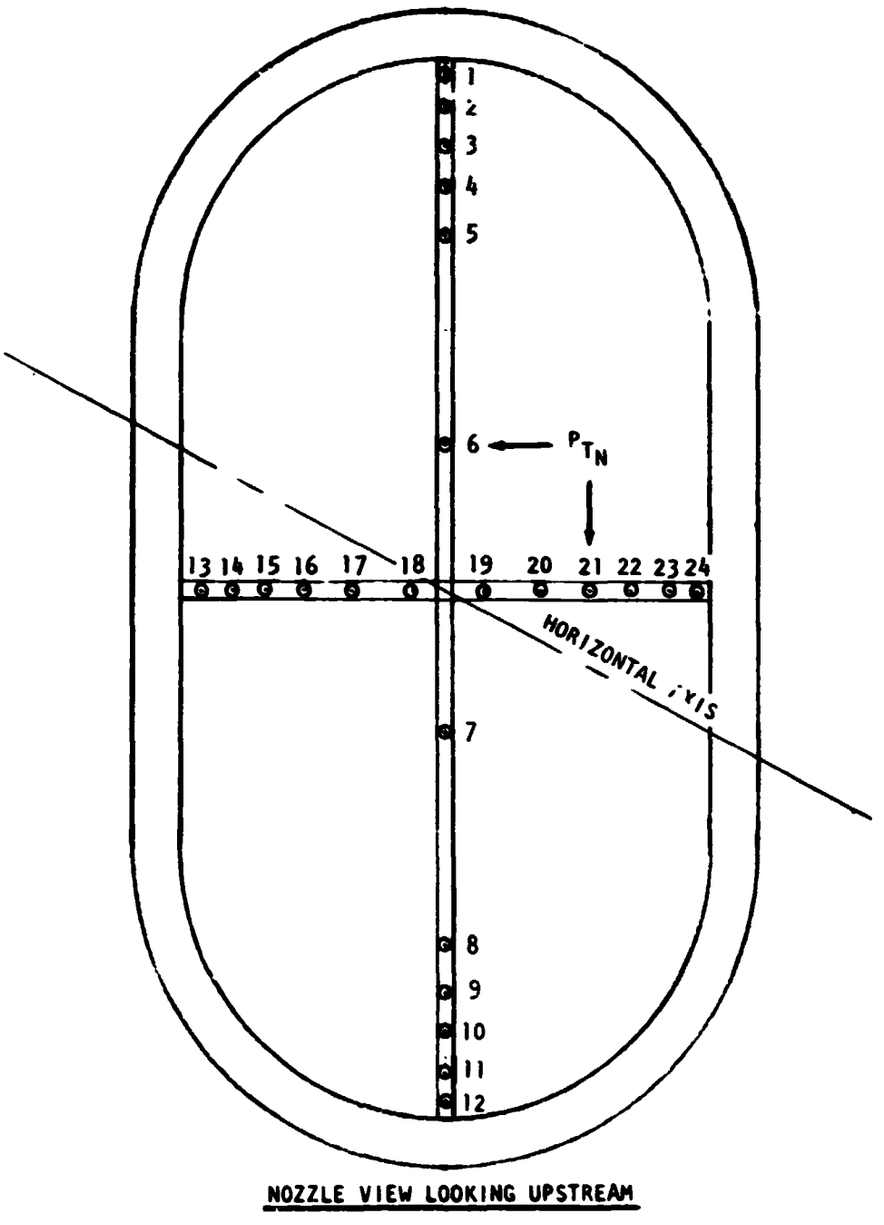

Figure 10. Exhaust Nozzle Rake For Total Pressures

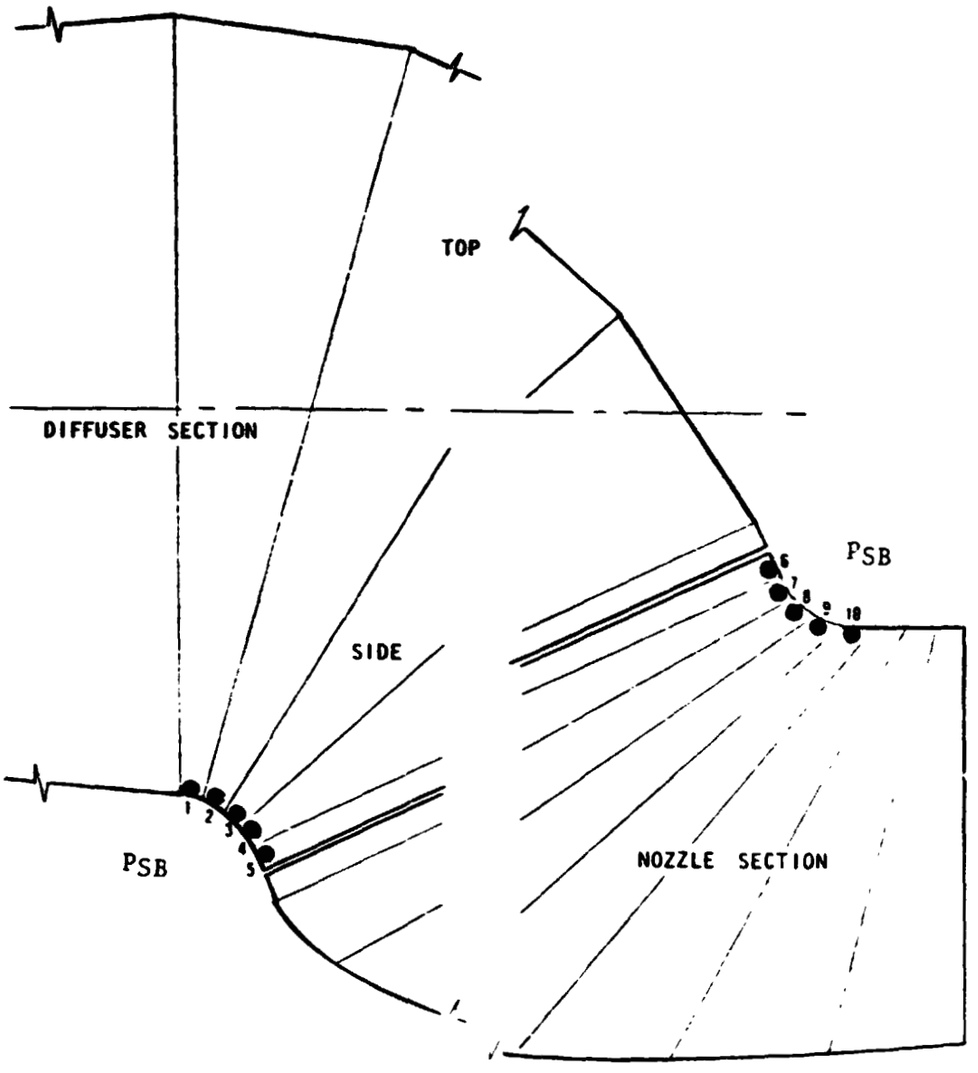

Figure 11. Static Pressure Tap Locations At Small Radius Bends

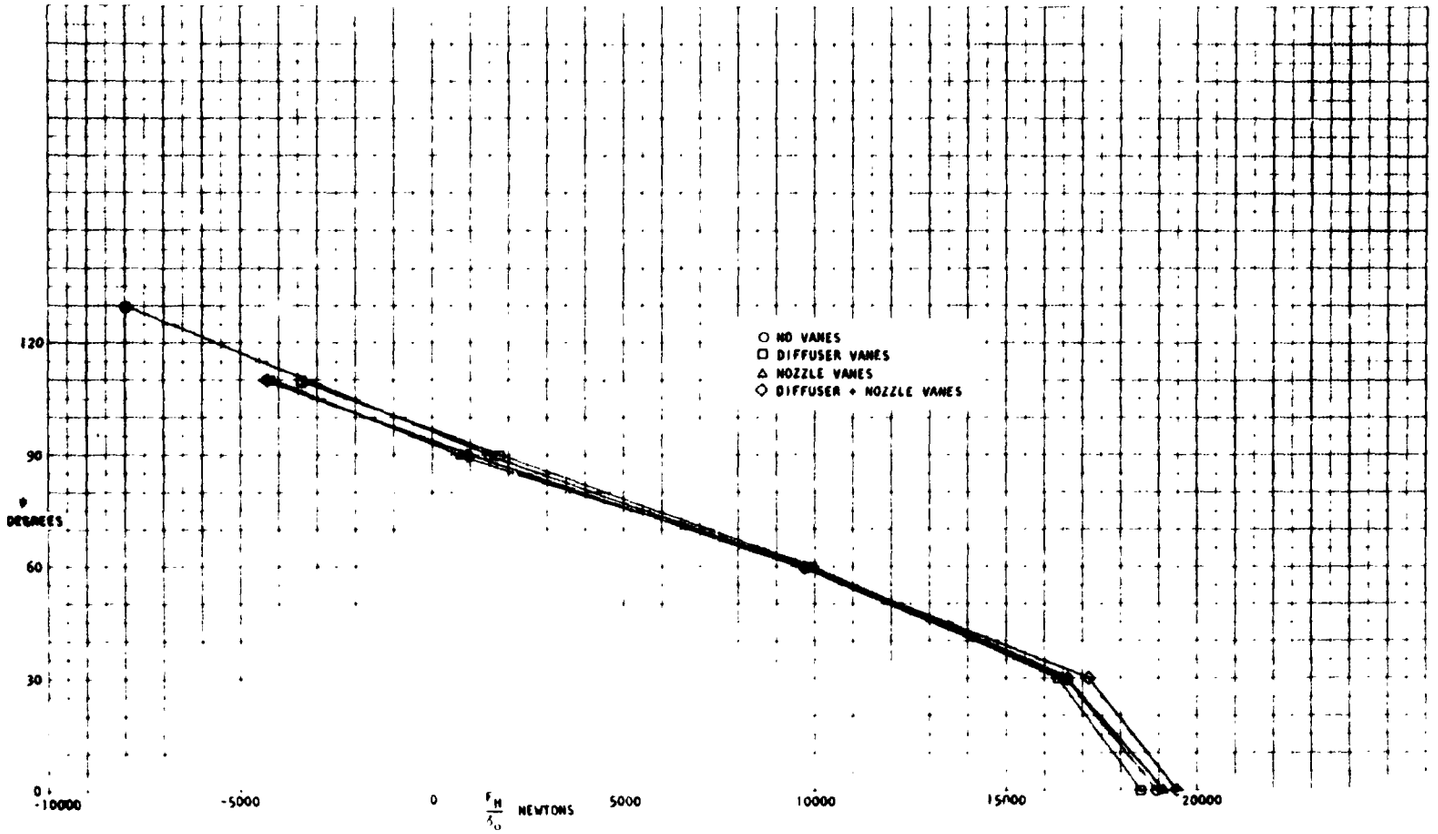

Figure 12 Deflector Nozzle Angle Vs Horizontal Thrust at 90% Fan Speed

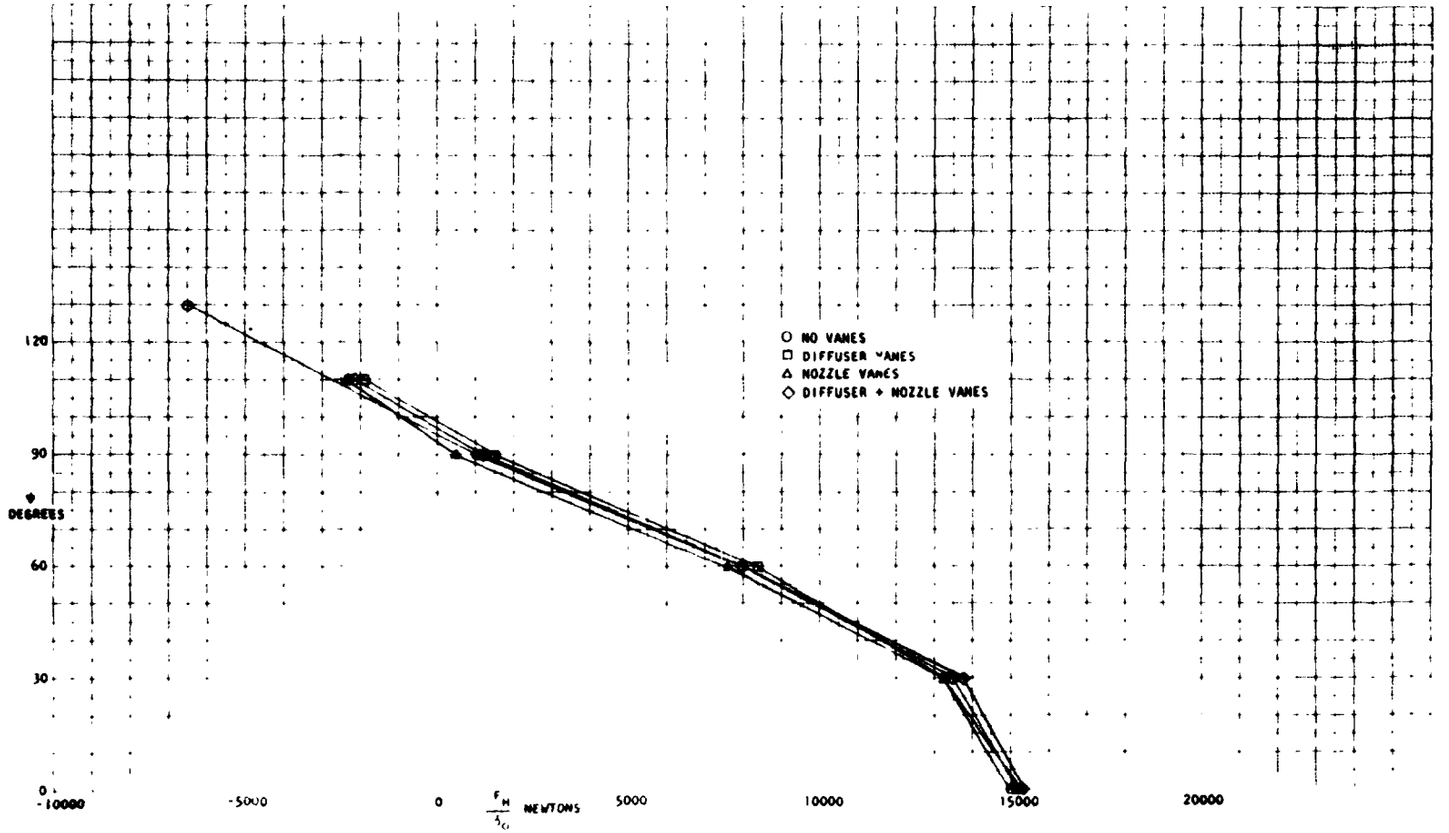

Figure 11 Deflector Nozzle Angle Vs Horizontal Thrust At 80% Fan Speed

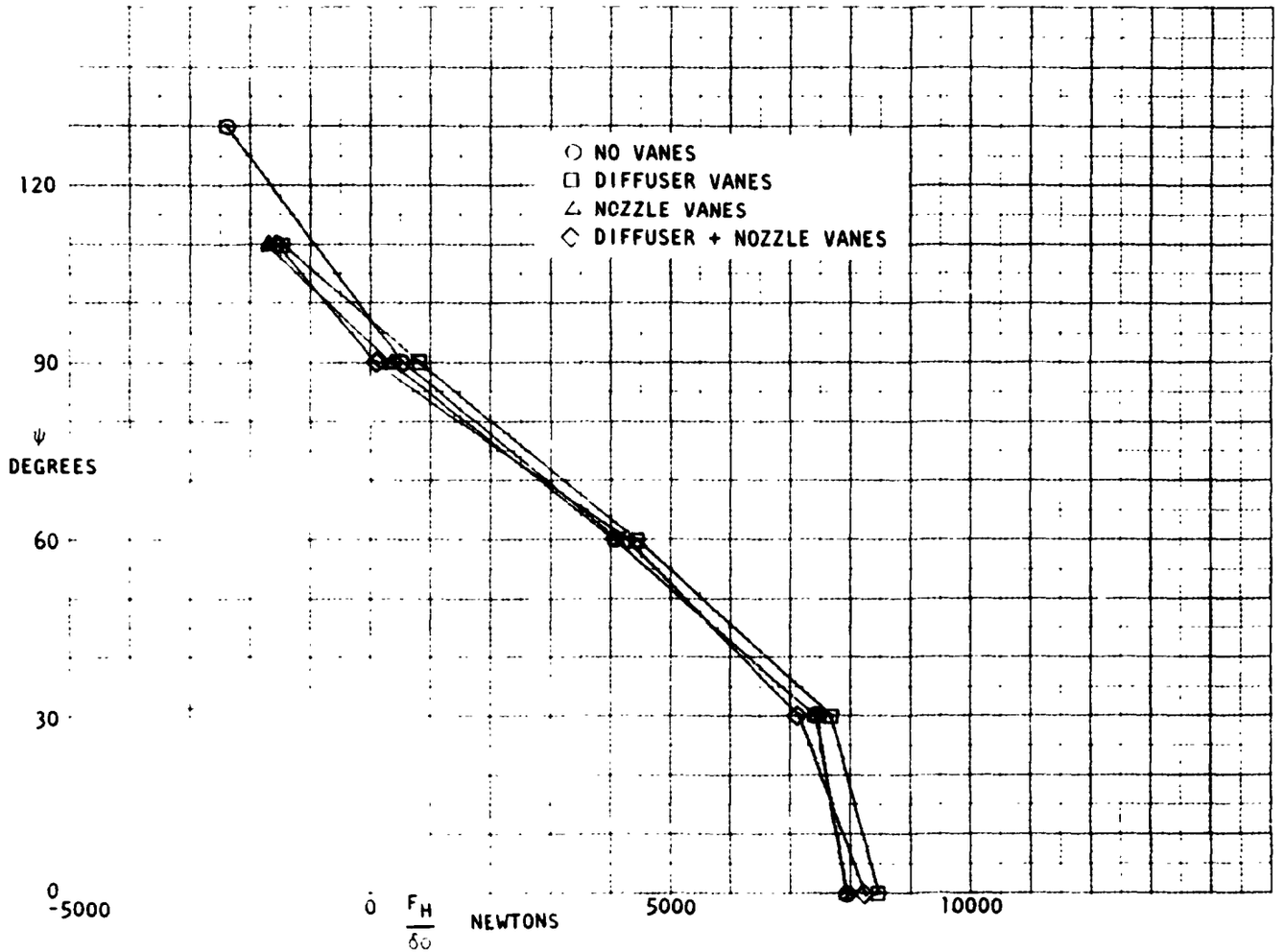

Figure 14. Deflector Nozzle Angle Vs. Horizontal Thrust At 60% Fan Speed

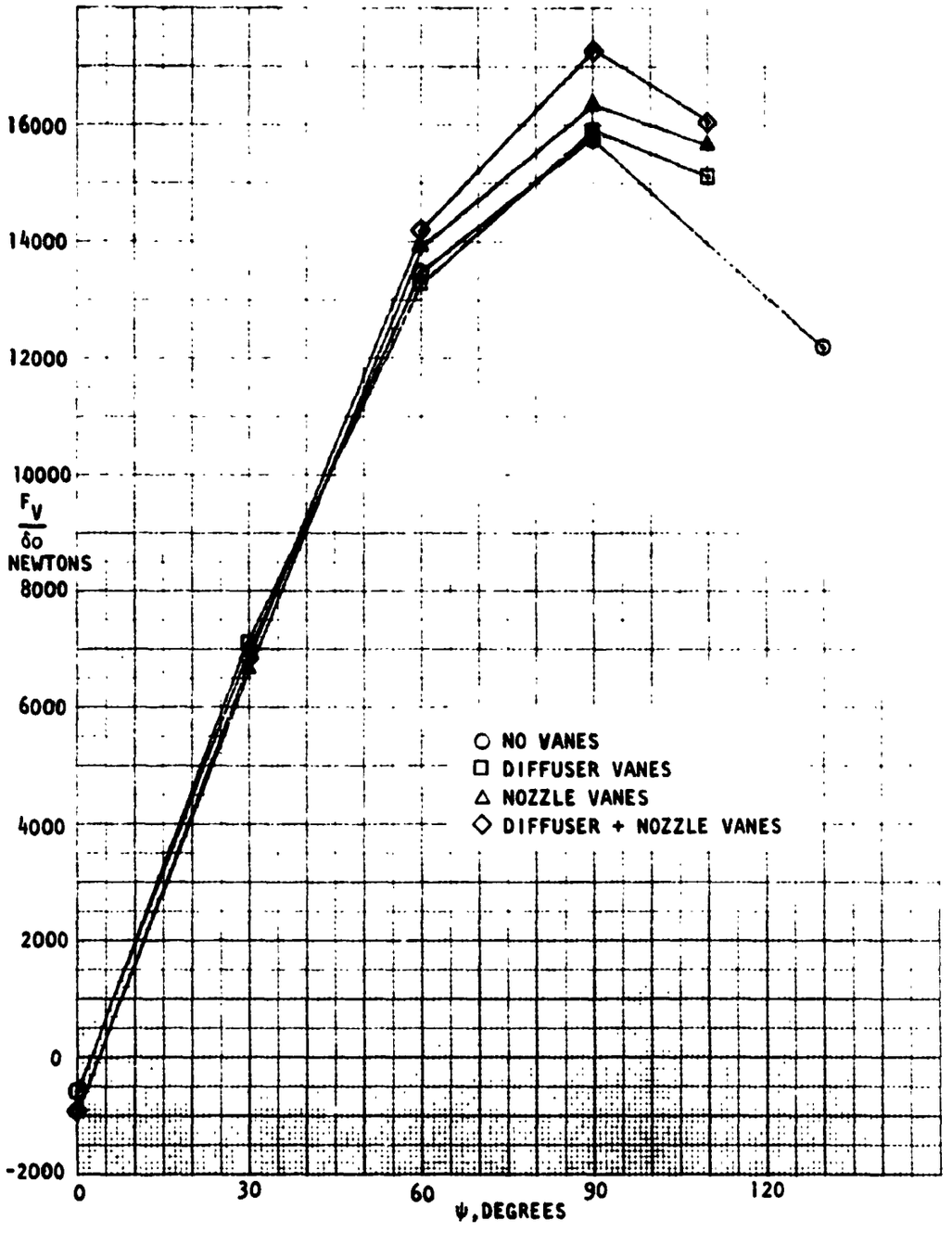

Figure 15. Vertical Thrust Vs. Deflector Nozzle Angle At 90% Fan Speed

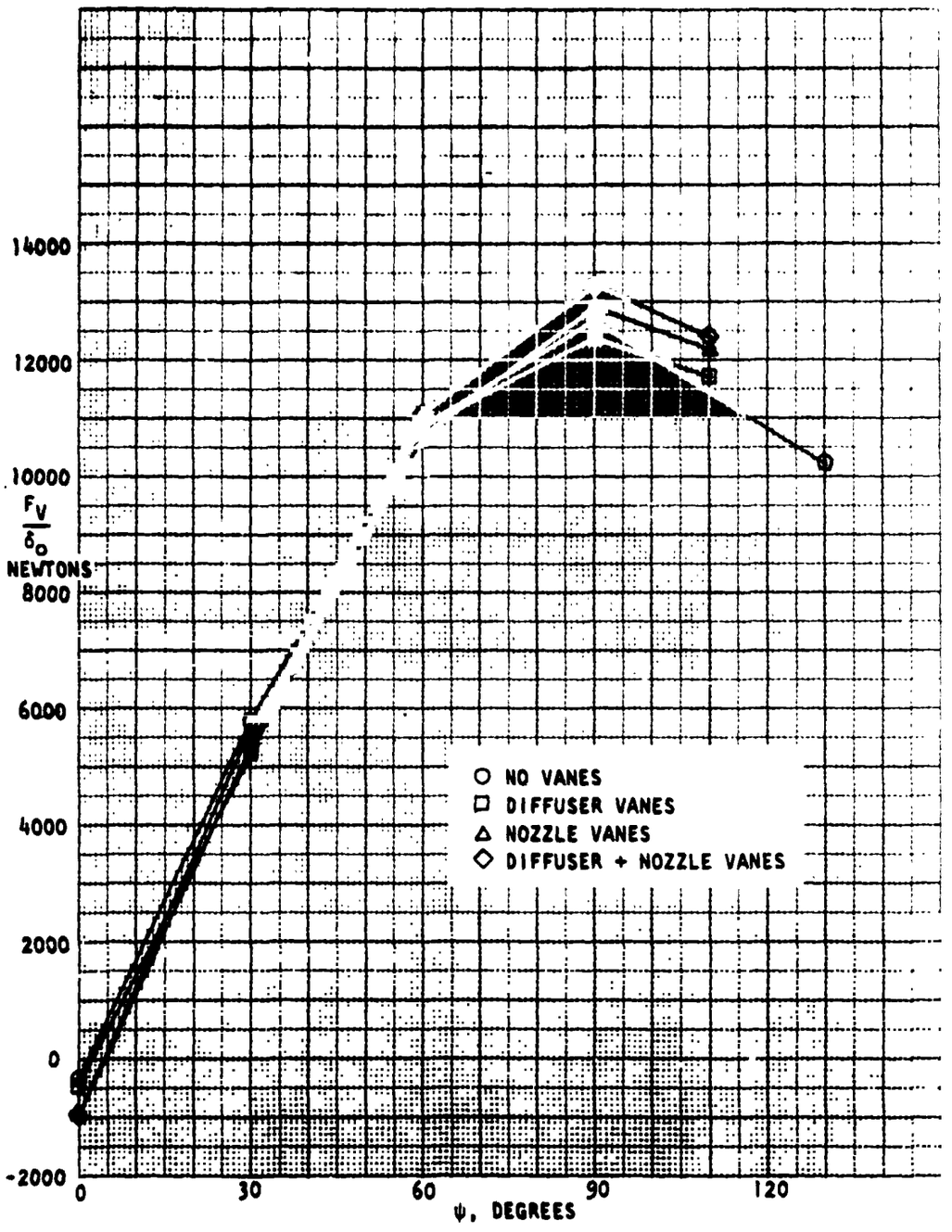

Figure 16. Vertical Thrust Vs. Deflector Nozzle Angle At 80% Fan Speed

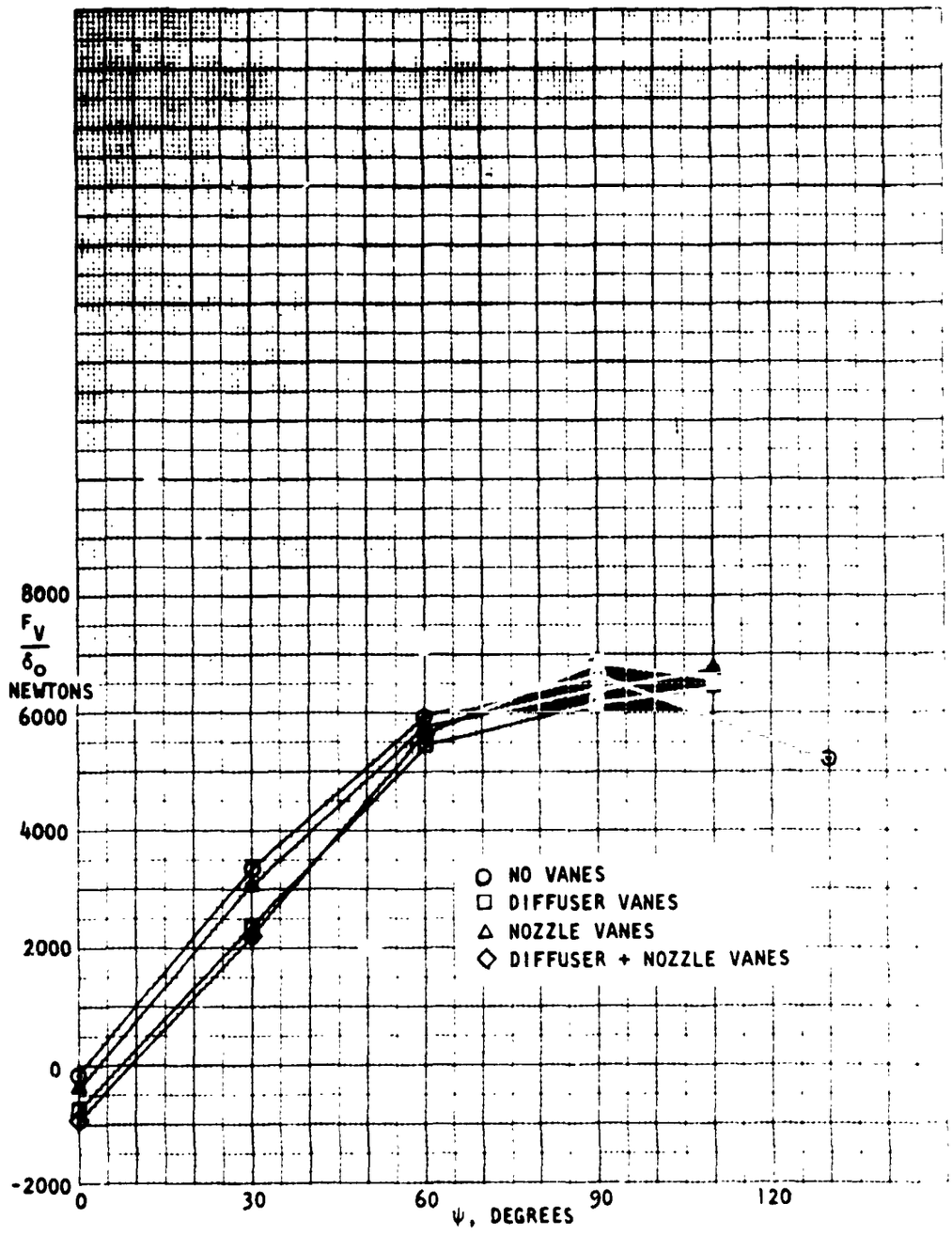

Figure 17. Vertical Thrust Vs. Deflector Nozzle Angle At 60% Fan Speed

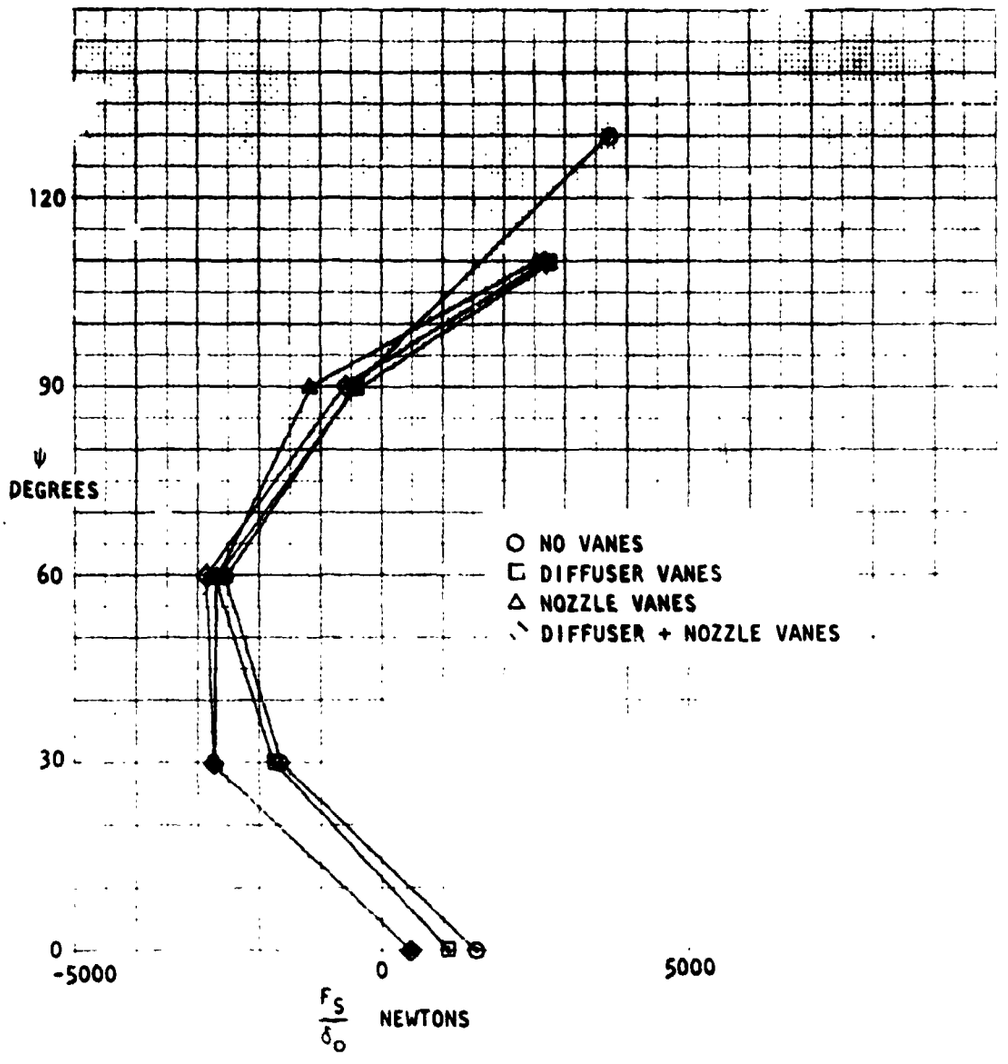

Figure 18. Deflector Nozzle Angle Vs. Side Thrust At 90% Fan Speed

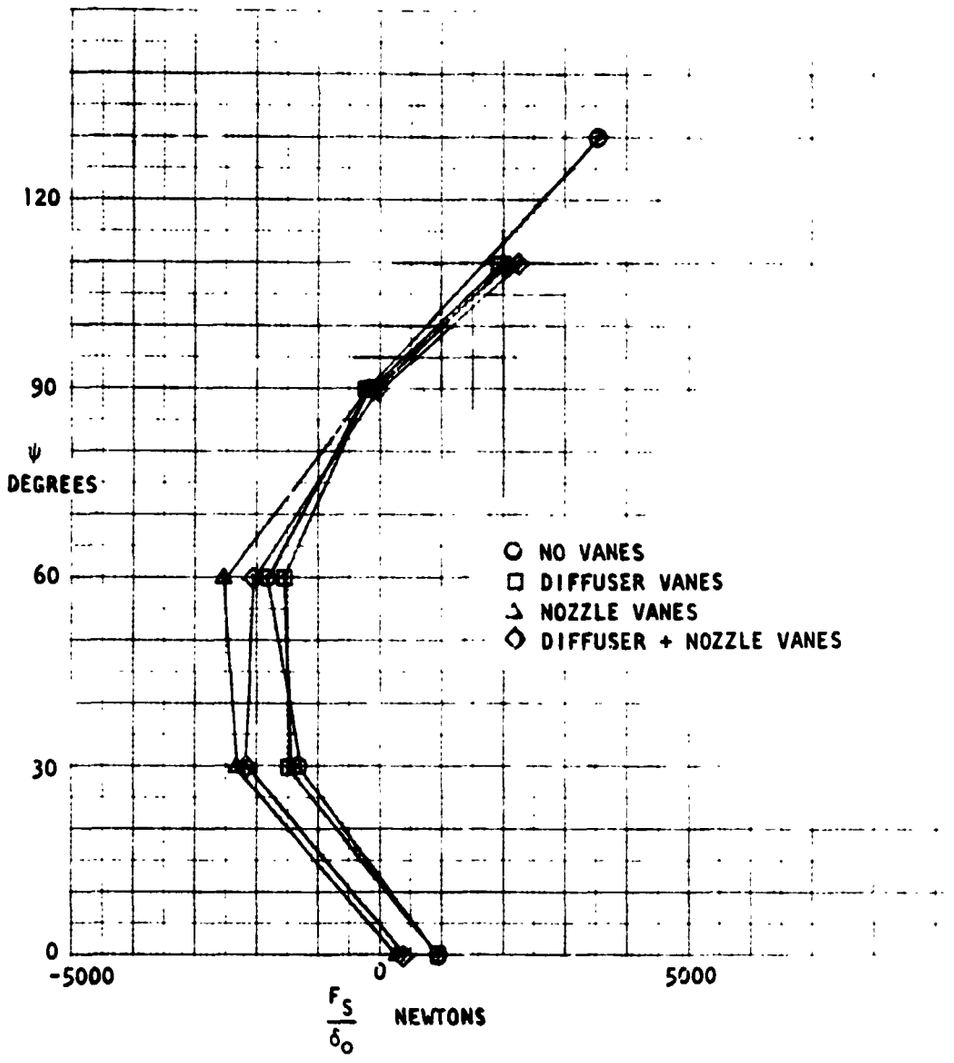

Figure 19. Deflector Nozzle Angle Vs. Side Thrust At 80% Fan Speed

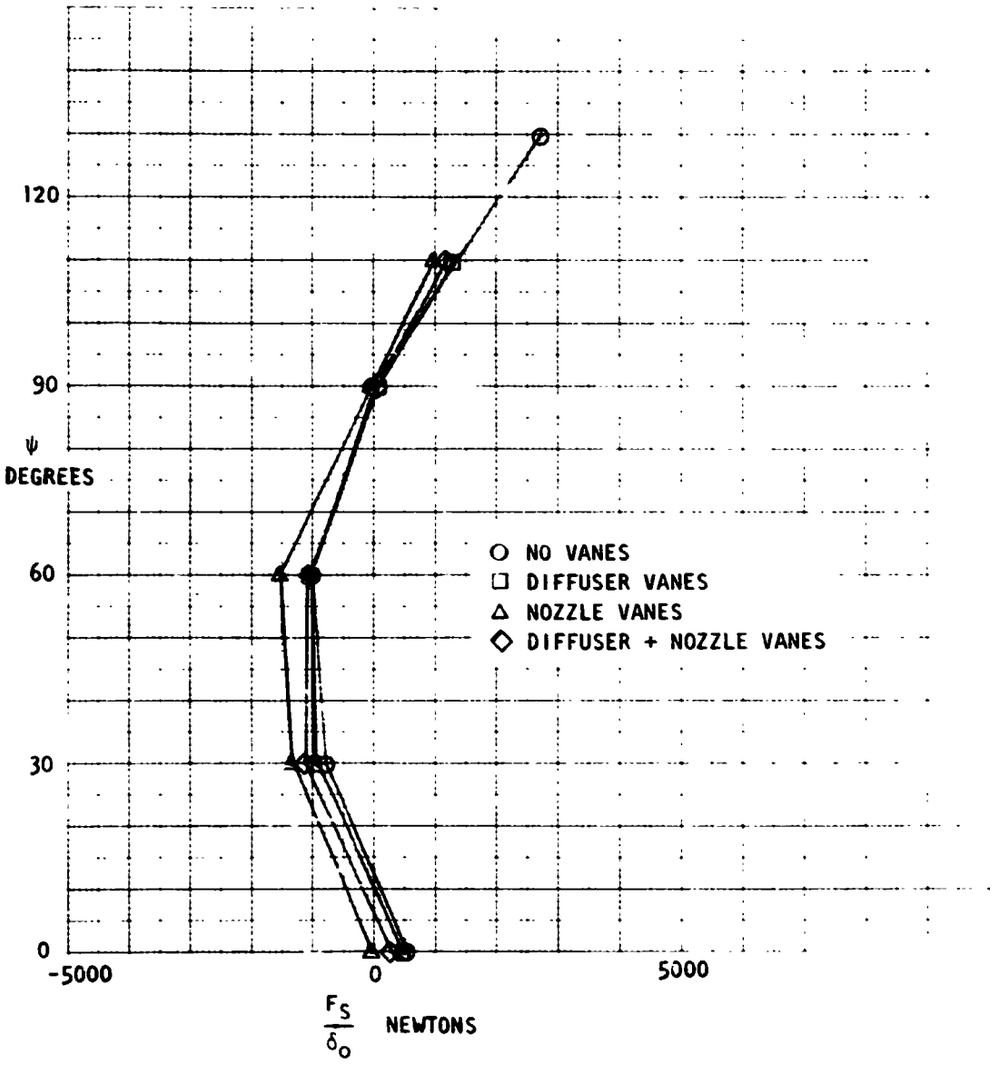

Figure 20. Deflector Nozzle Angle Vs. Side Thrust At 60% Fan Speed

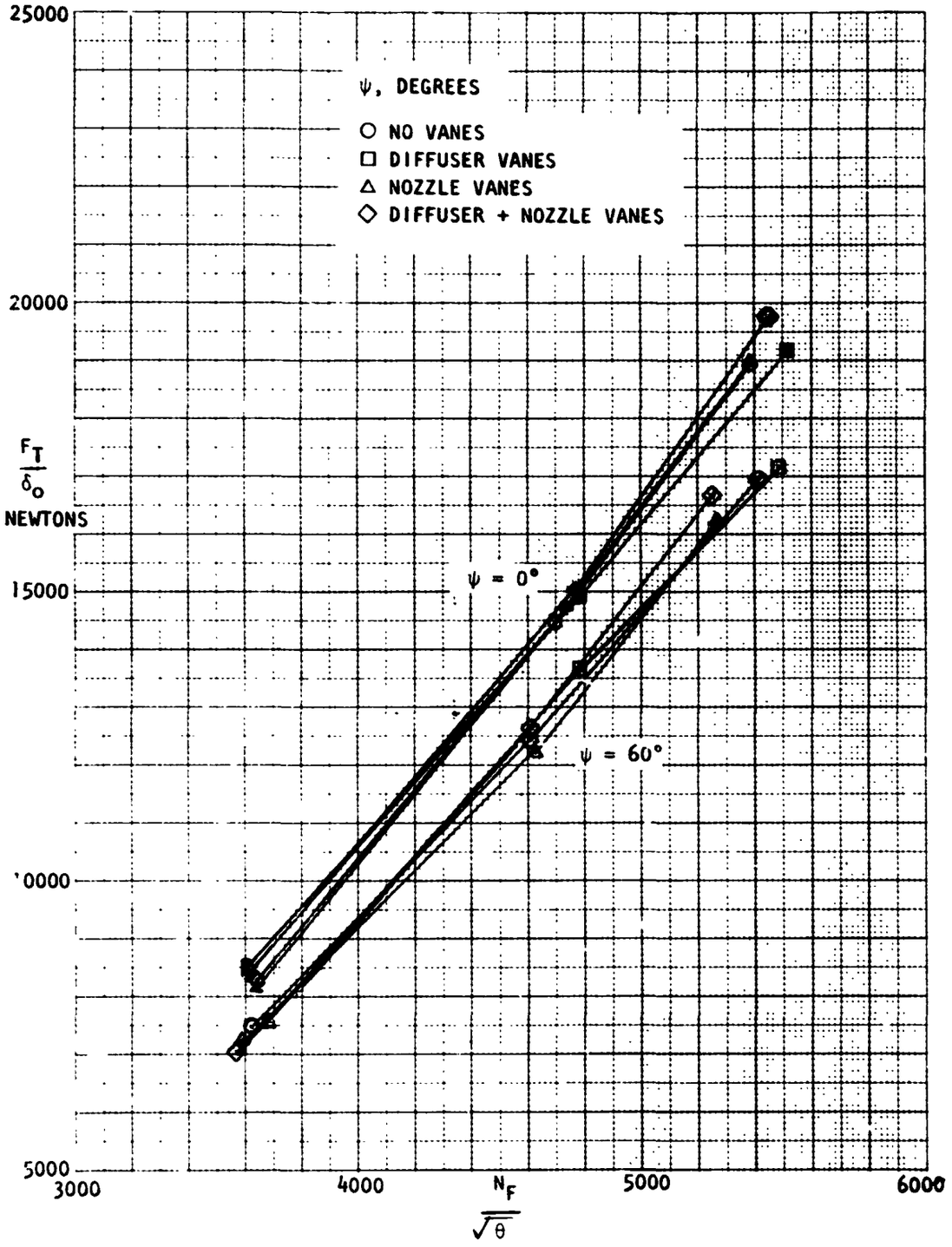

Figure 21. Total Thrust Vs. Fan Speed at 0° and 60° Nozzle Angle

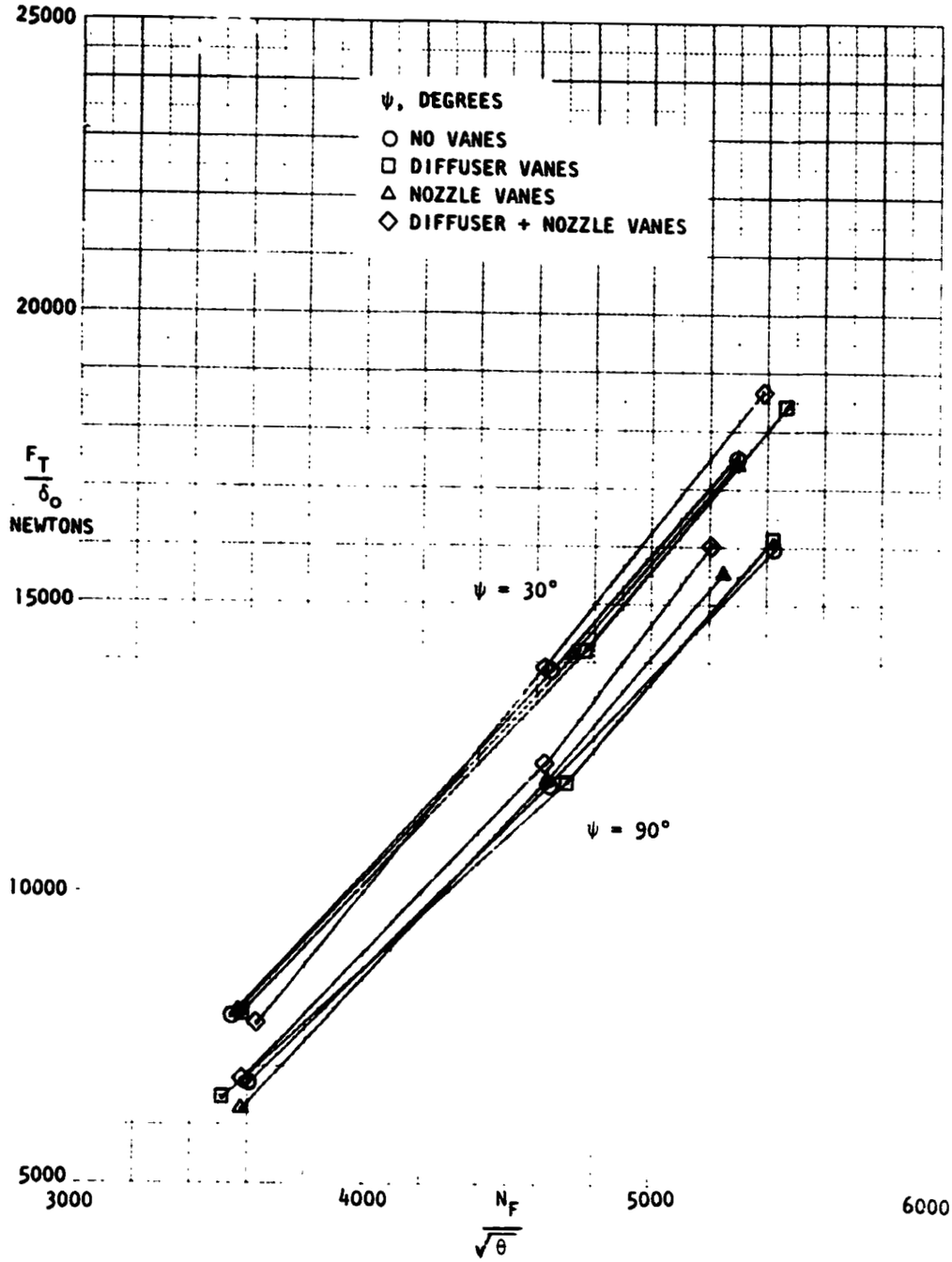

Figure 22. Total Thrust Vs. Fan Speed At 30° and 90° Nozzle Angle

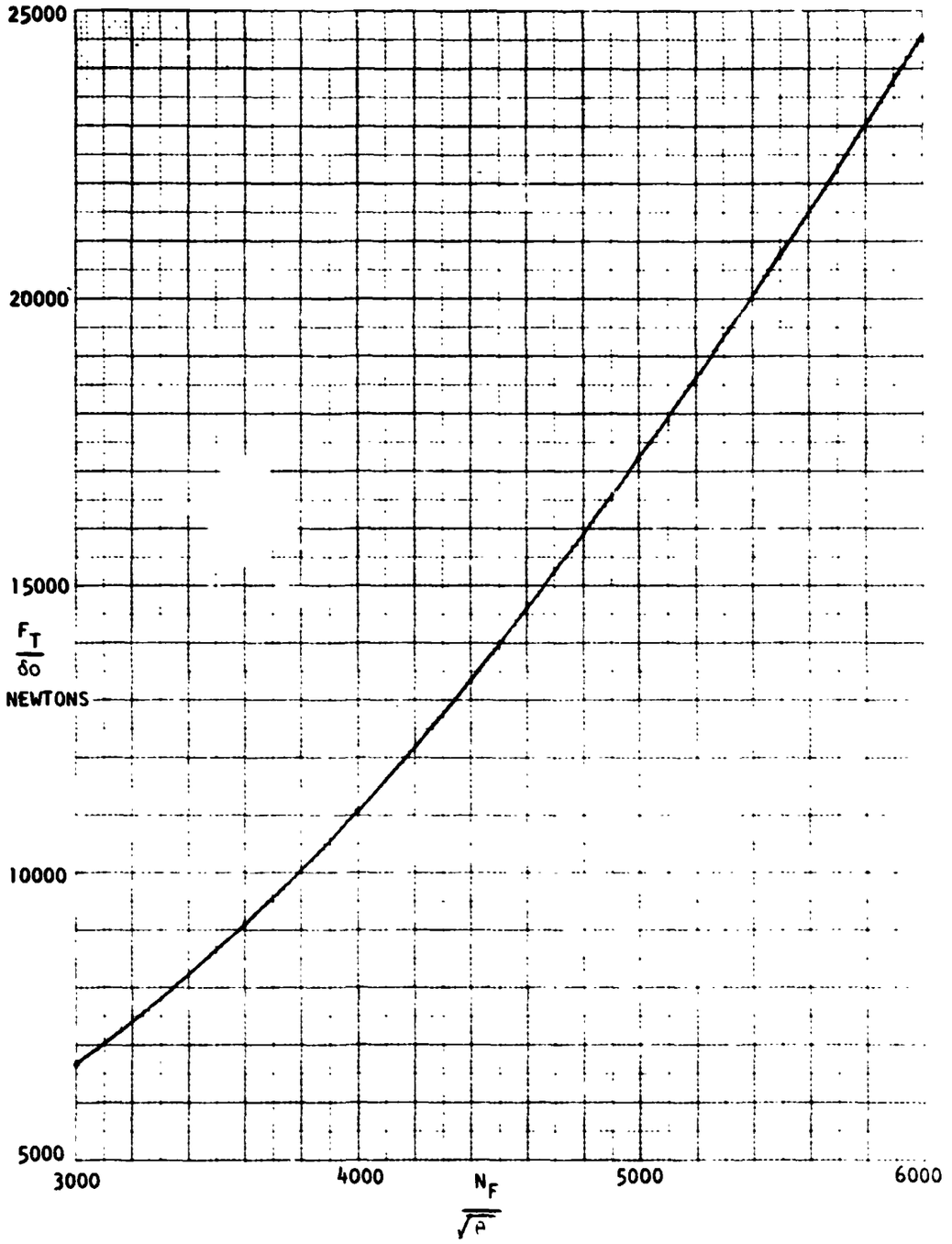

Figure 23. LF336/A Lift Fan Performance Calibrated Test Data

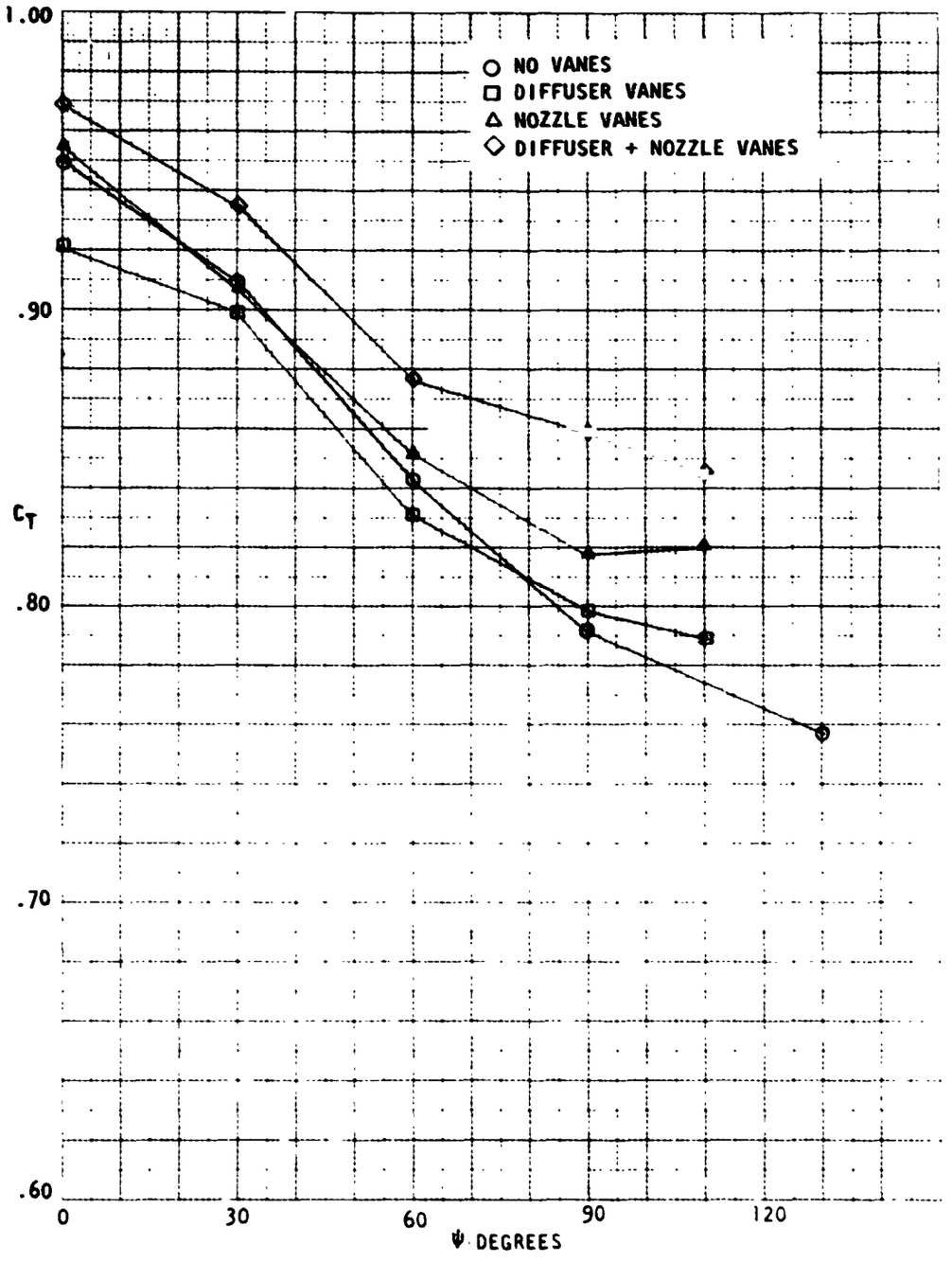

Figure 24. Thrust Coefficient Vs. Deflector Nozzle Angle At 90% Fan Speed

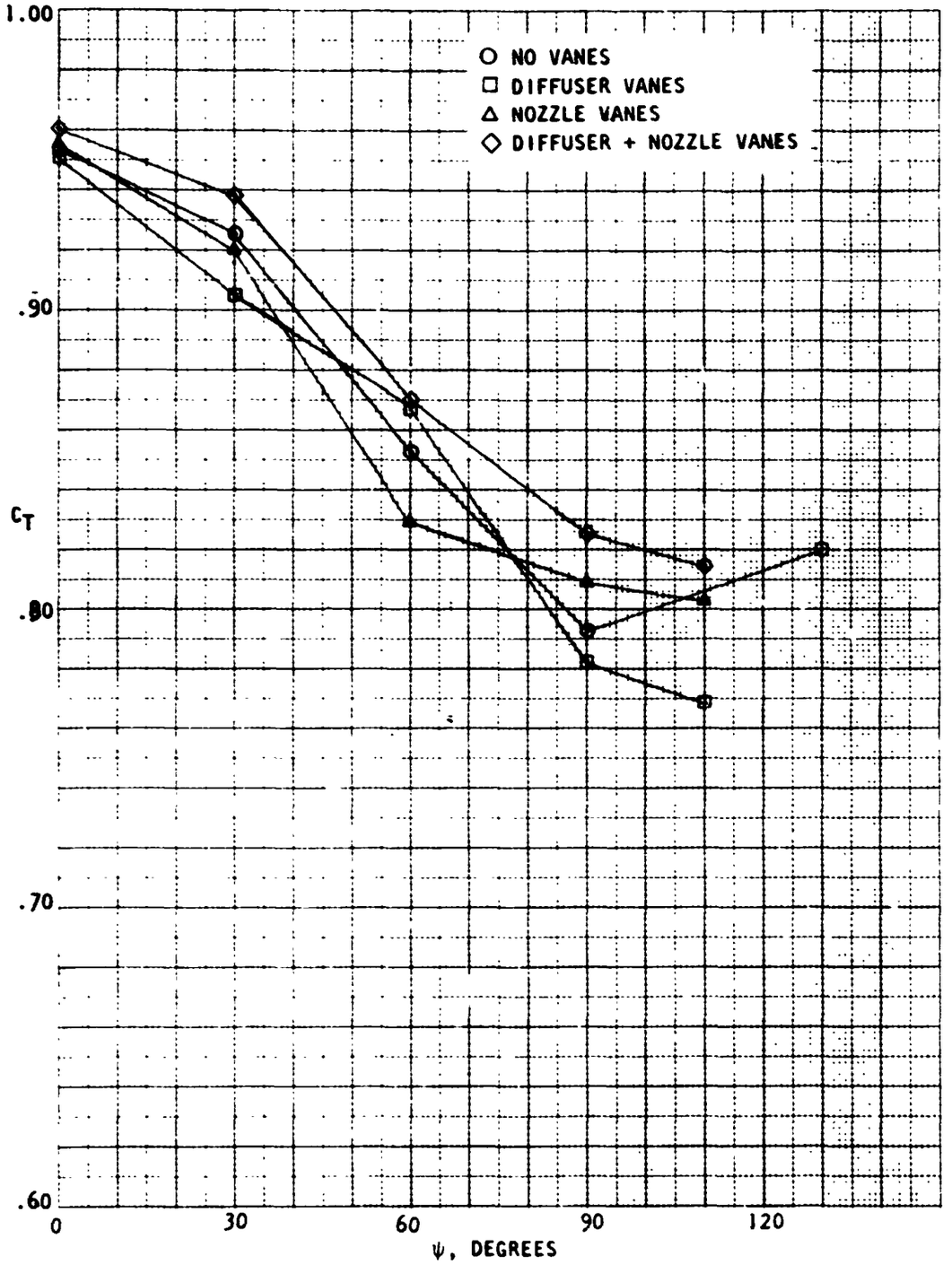

Figure 25. Thrust Coefficient Vs. Deflector Nozzle Angle At 80% Fan Speed

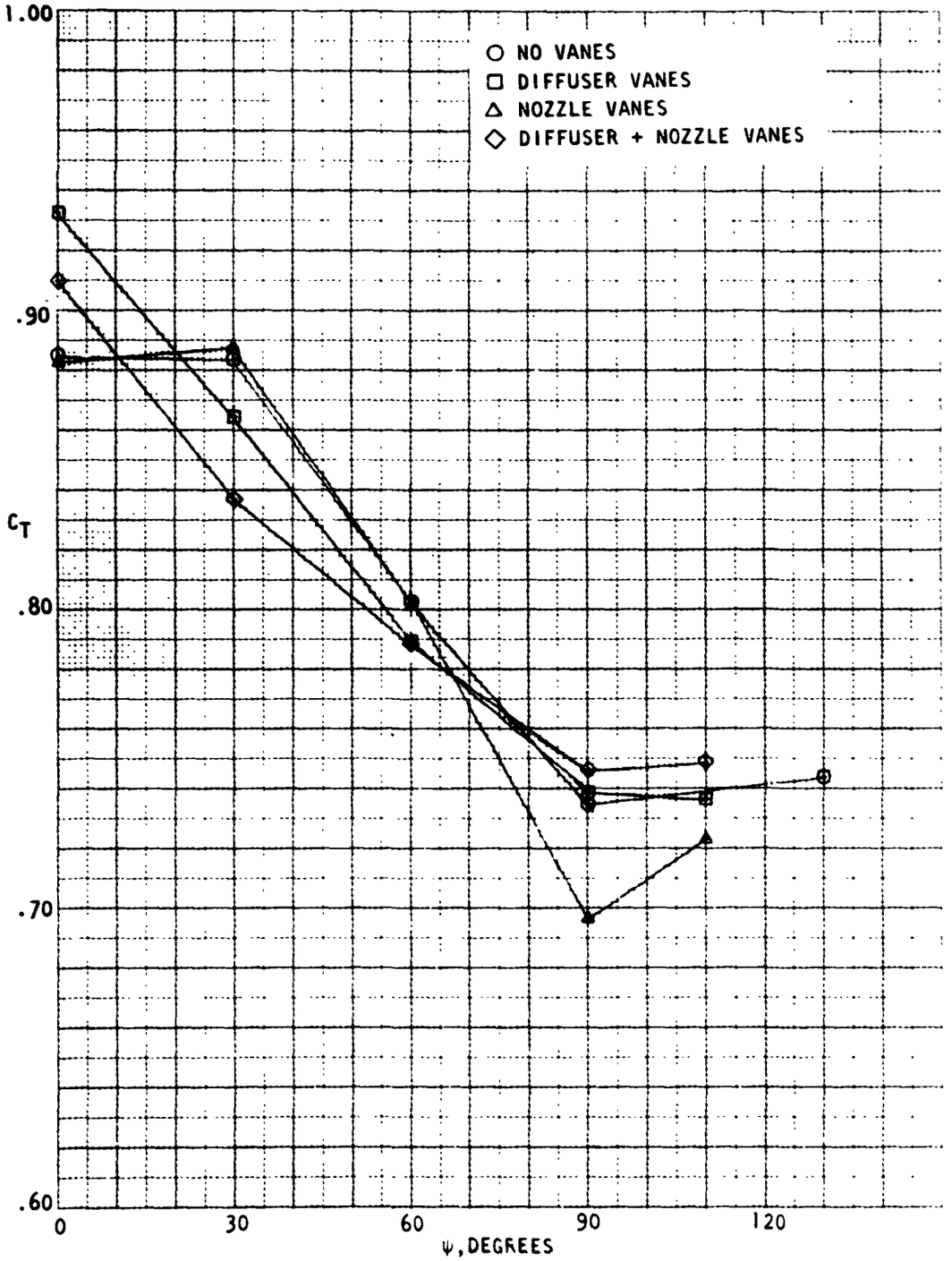

Figure 26. Thrust Coefficient Vs. Deflector Nozzle Angle At 60% Fan Speed

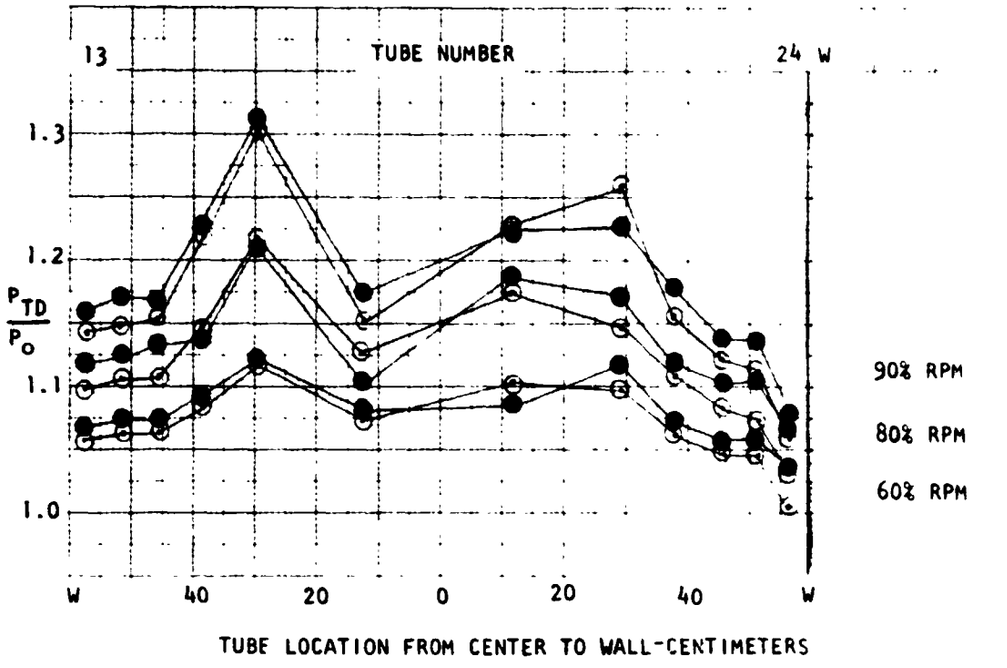

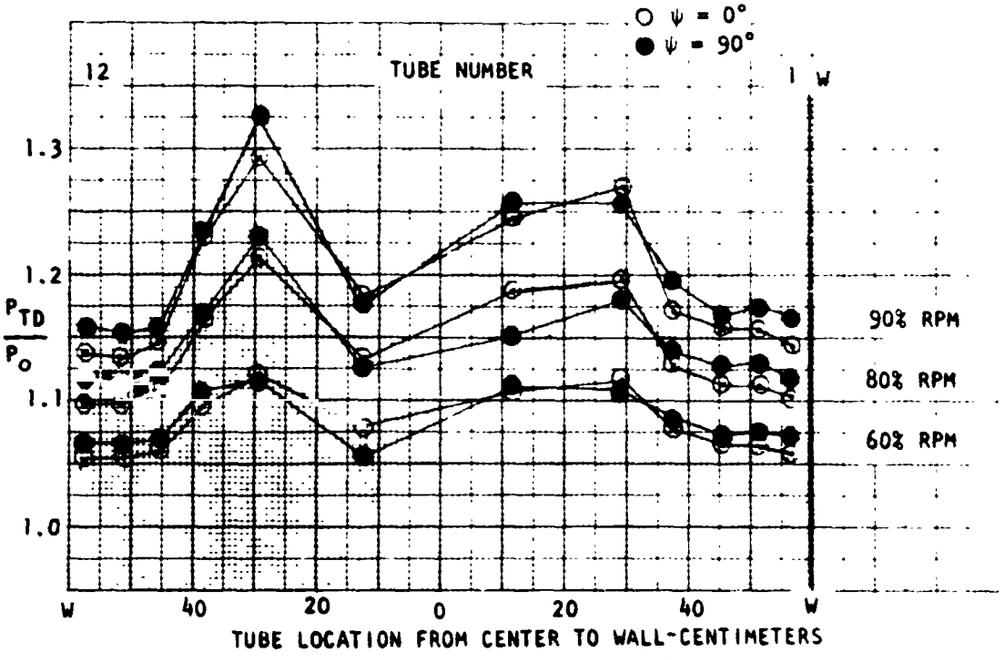

Figure 27. Diffuser Exit Total Pressure Ratio Vs. Tube Location For 90%, 80% and 60% Fan Speed

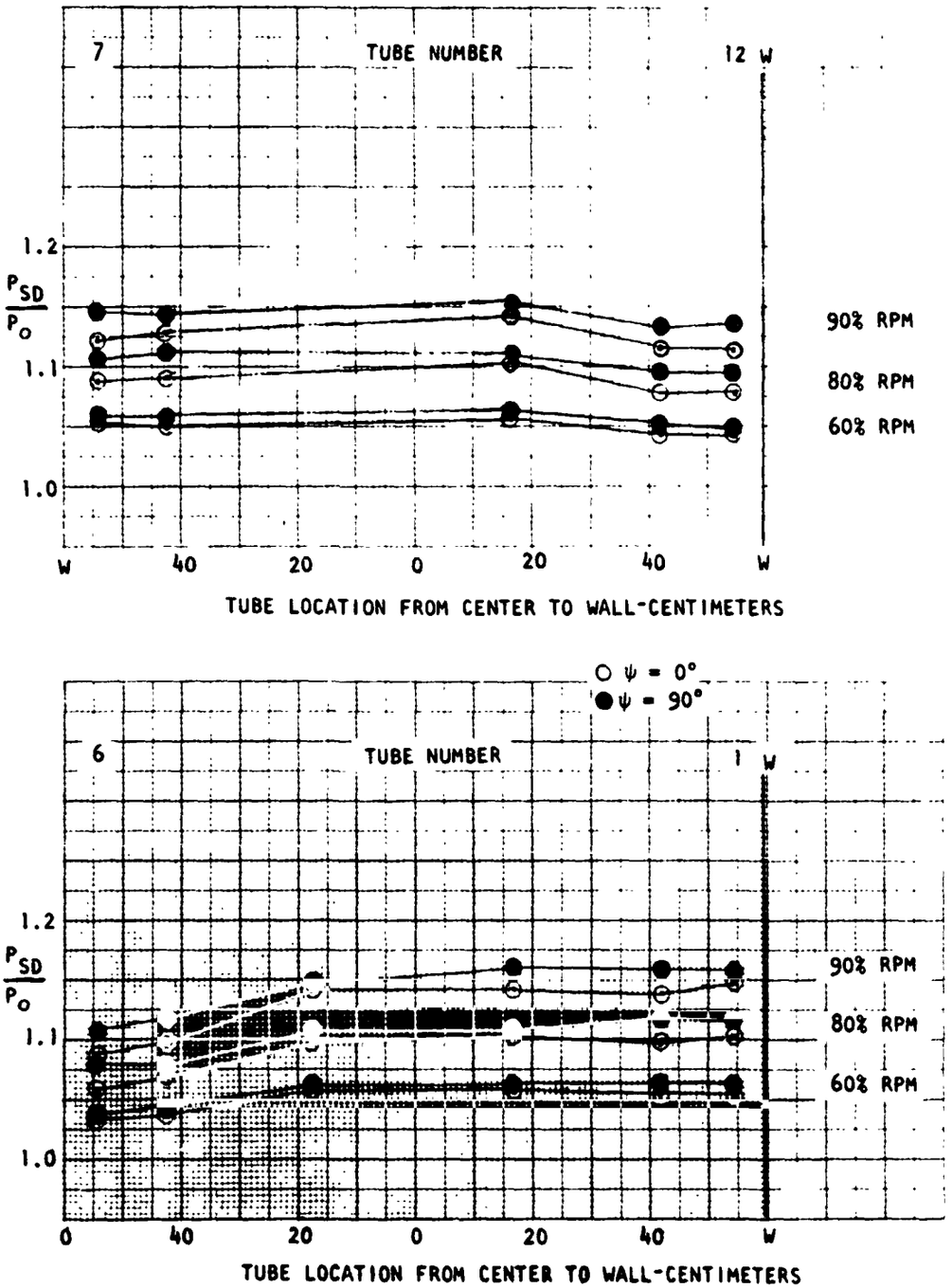

Figure 28. Diffuser Exit Static Pressure Ratio Vs. Tube Location for 90%, 80% and 60% Fan Speed

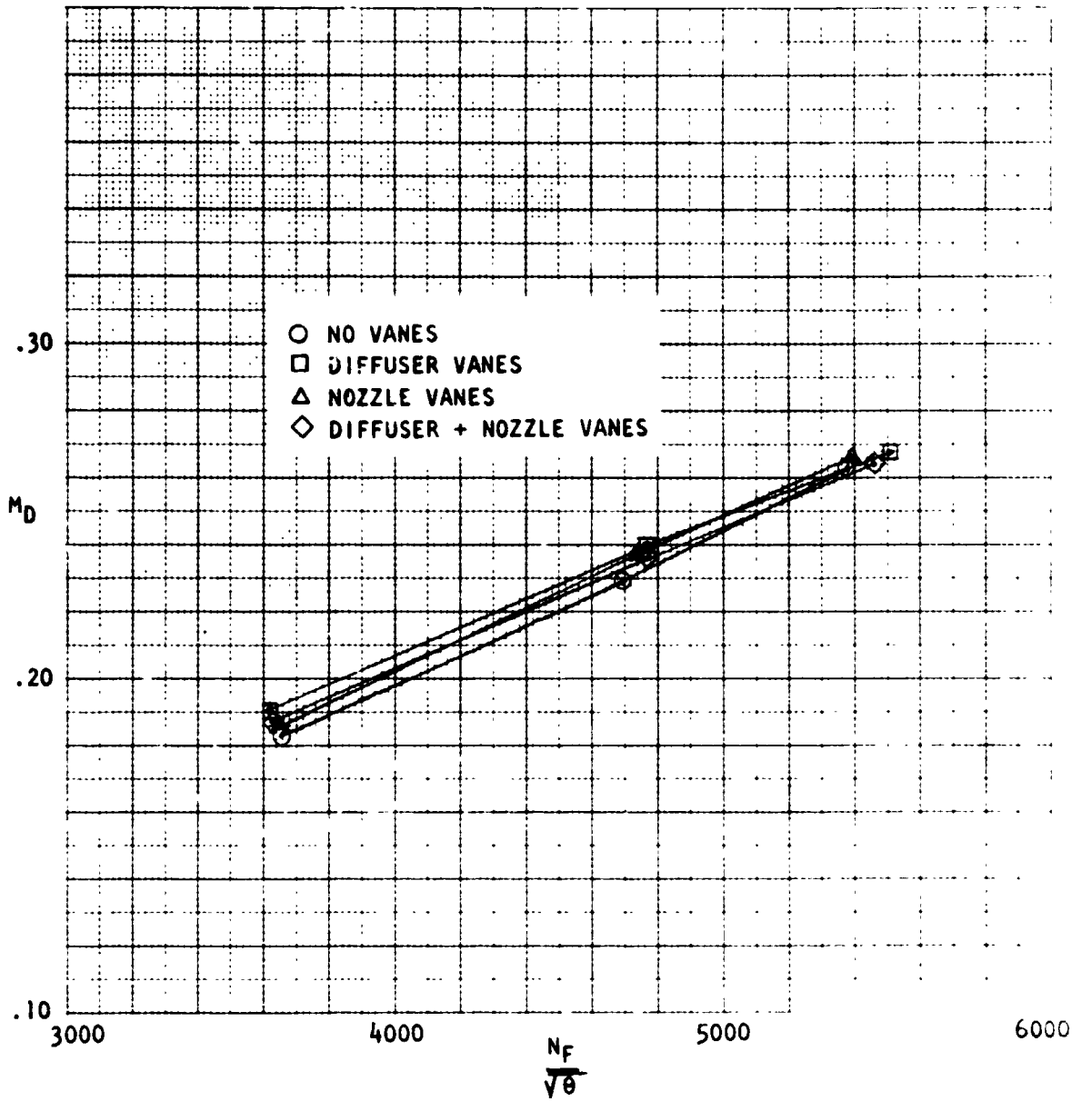

Figure 29. Duct Mach Number Vs. Fan Speed At 0° Nozzle Angle

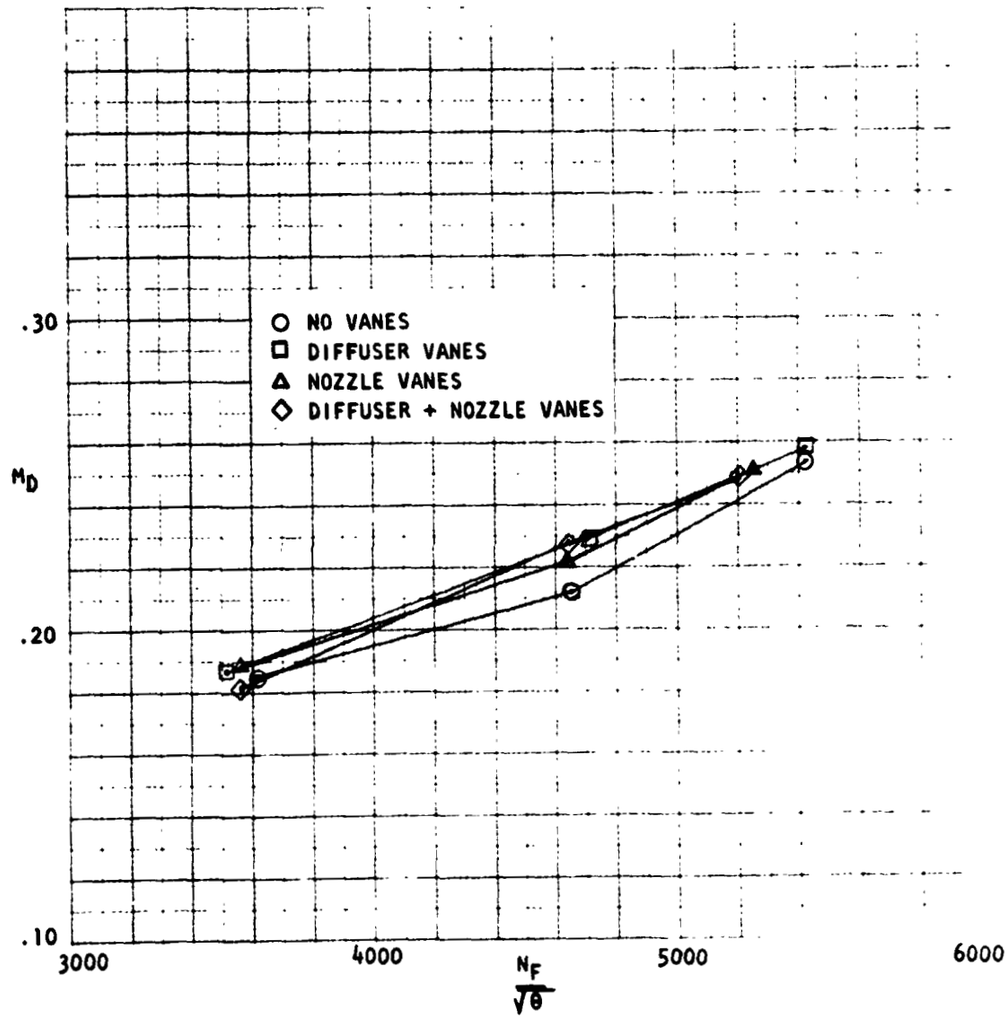

Figure 30. Duct Mach Number Vs. Fan Speed at 90° Nozzle Angle

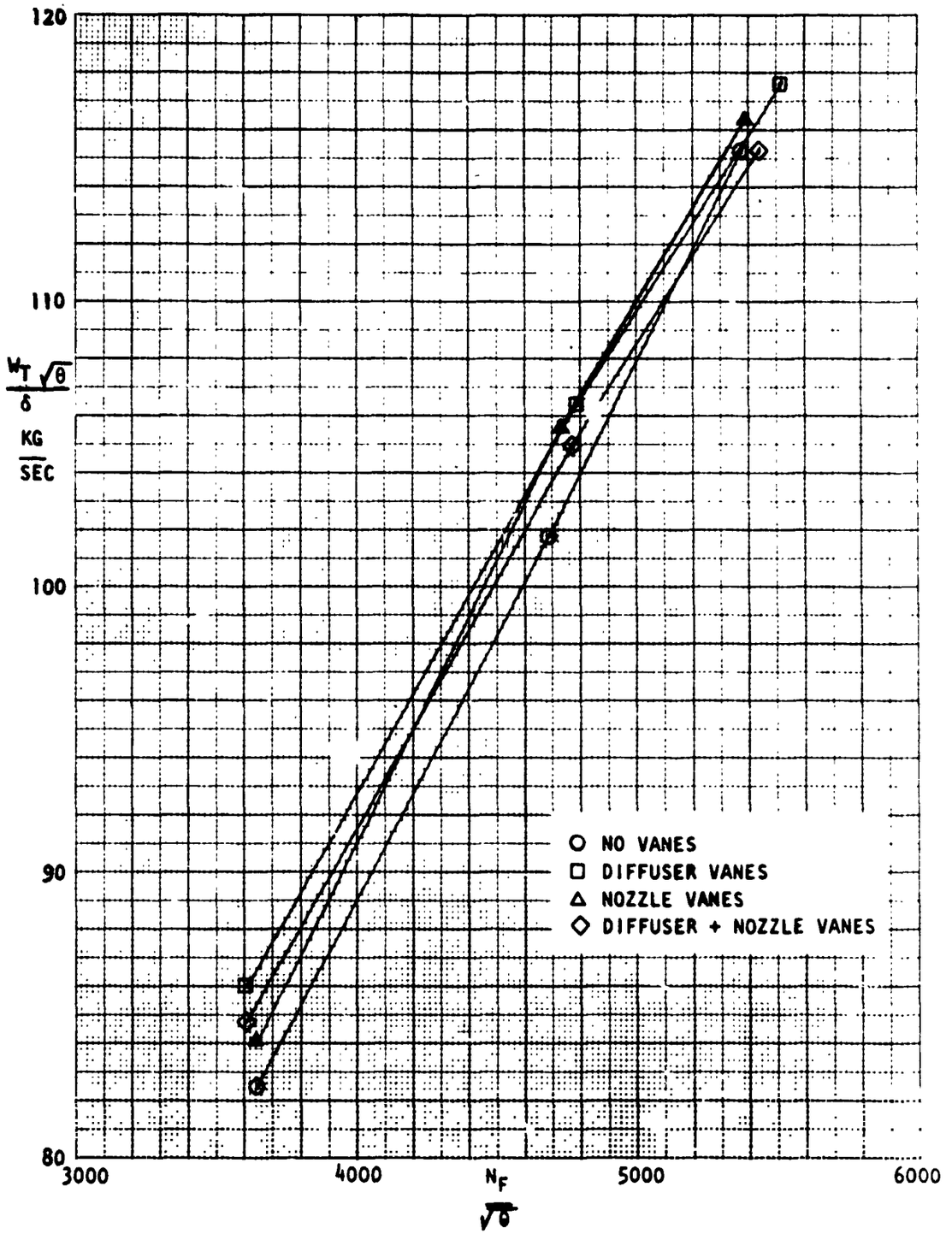

Figure 31. Total Exhaust Flow Vs. Fan Speed At 0° Nozzle Angle

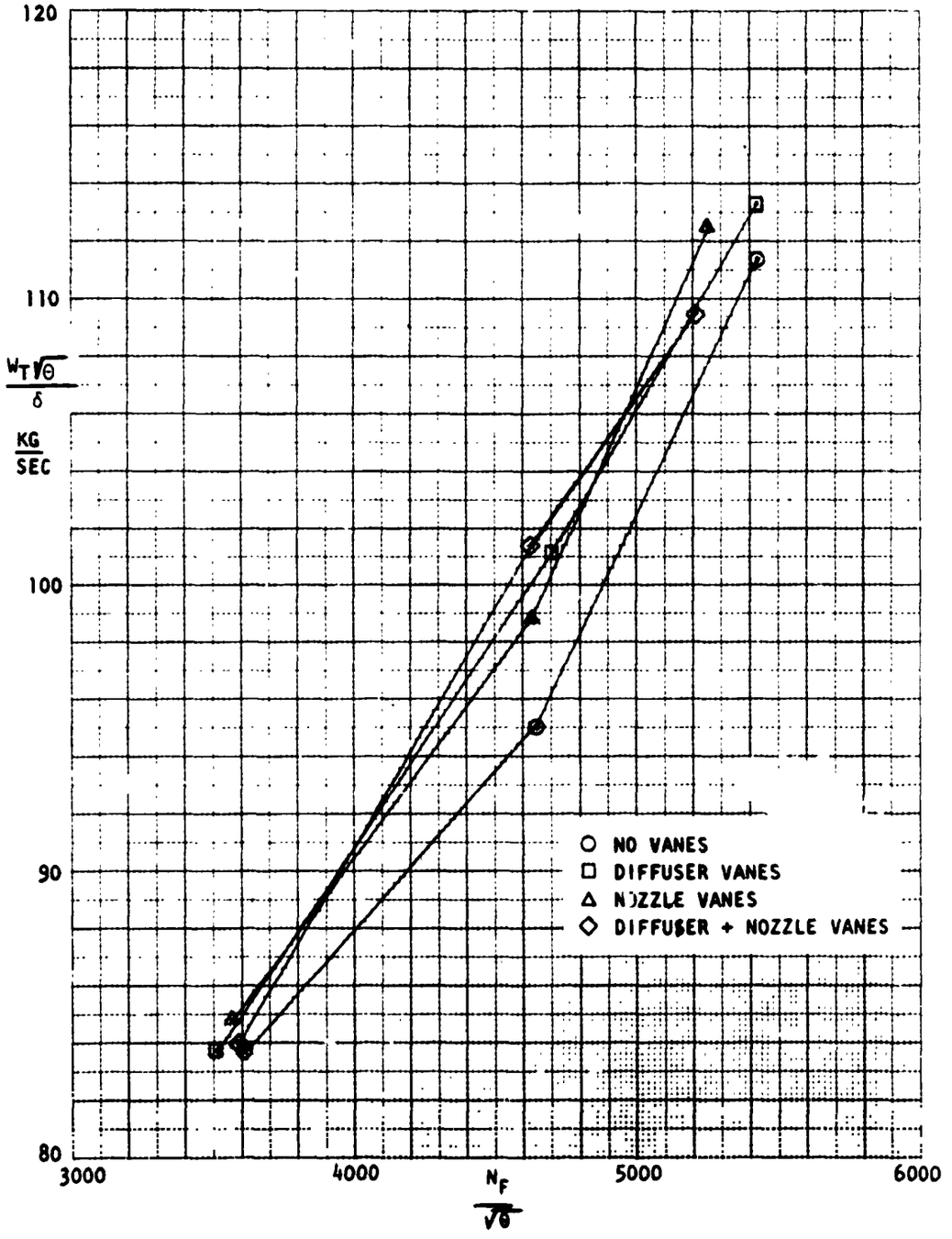

Figure 32. Total Exhaust Flow Vs. Fan Speed At 90° Nozzle Angle

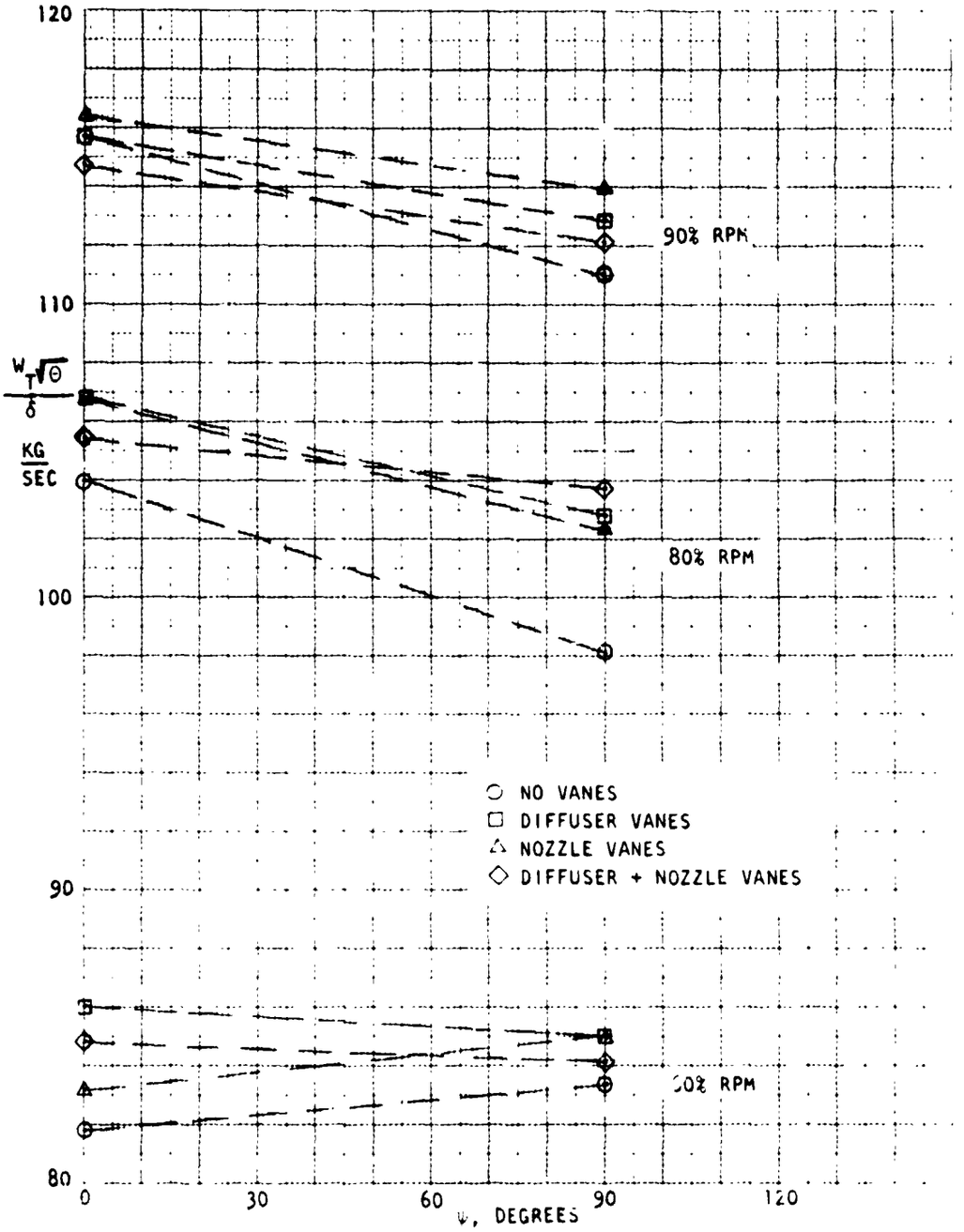

Figure 33. Total Exhaust Flow Vs. Deflector Nozzle Angle At 90%, 80% and 60% Fan Speed

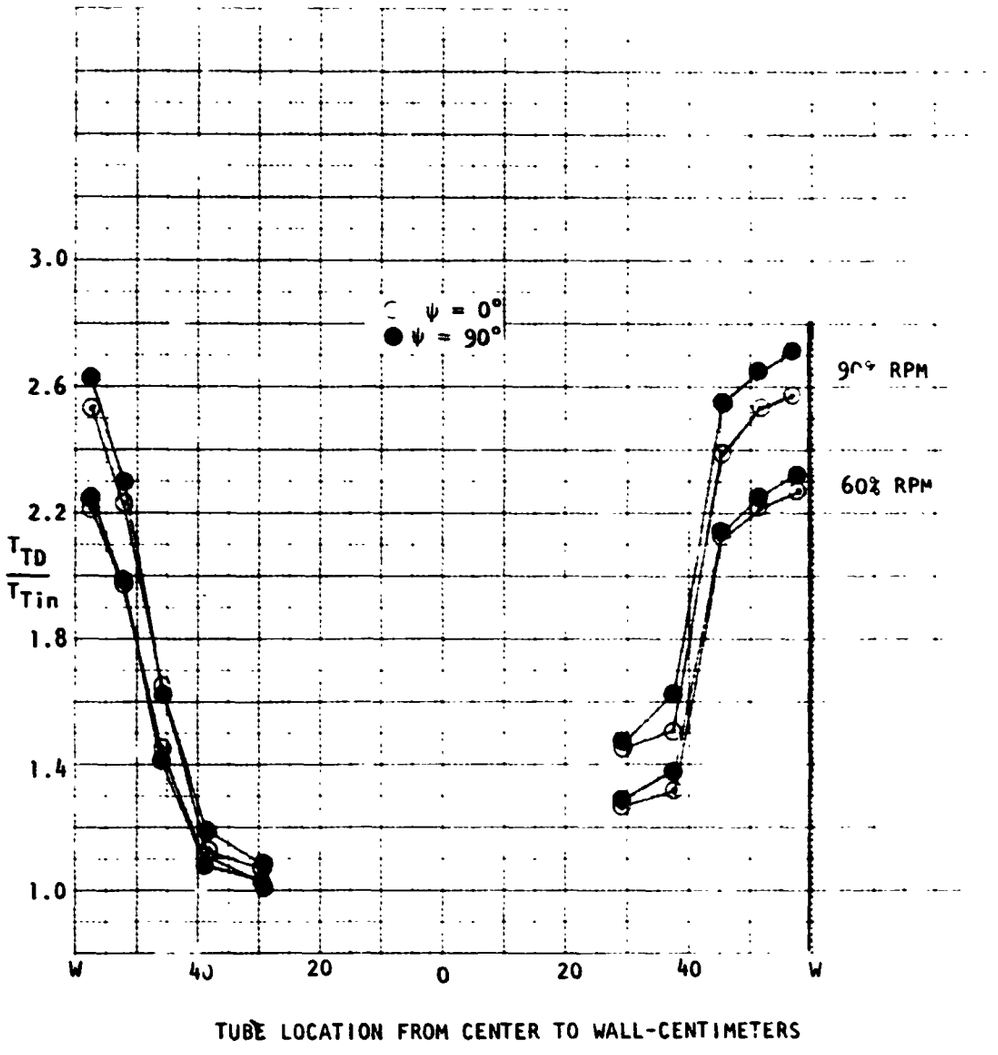

Figure 34. Diffuser Exit Total Temperature Ratio vs. Temperature Tube Location for 90% and 60% Fan Speed

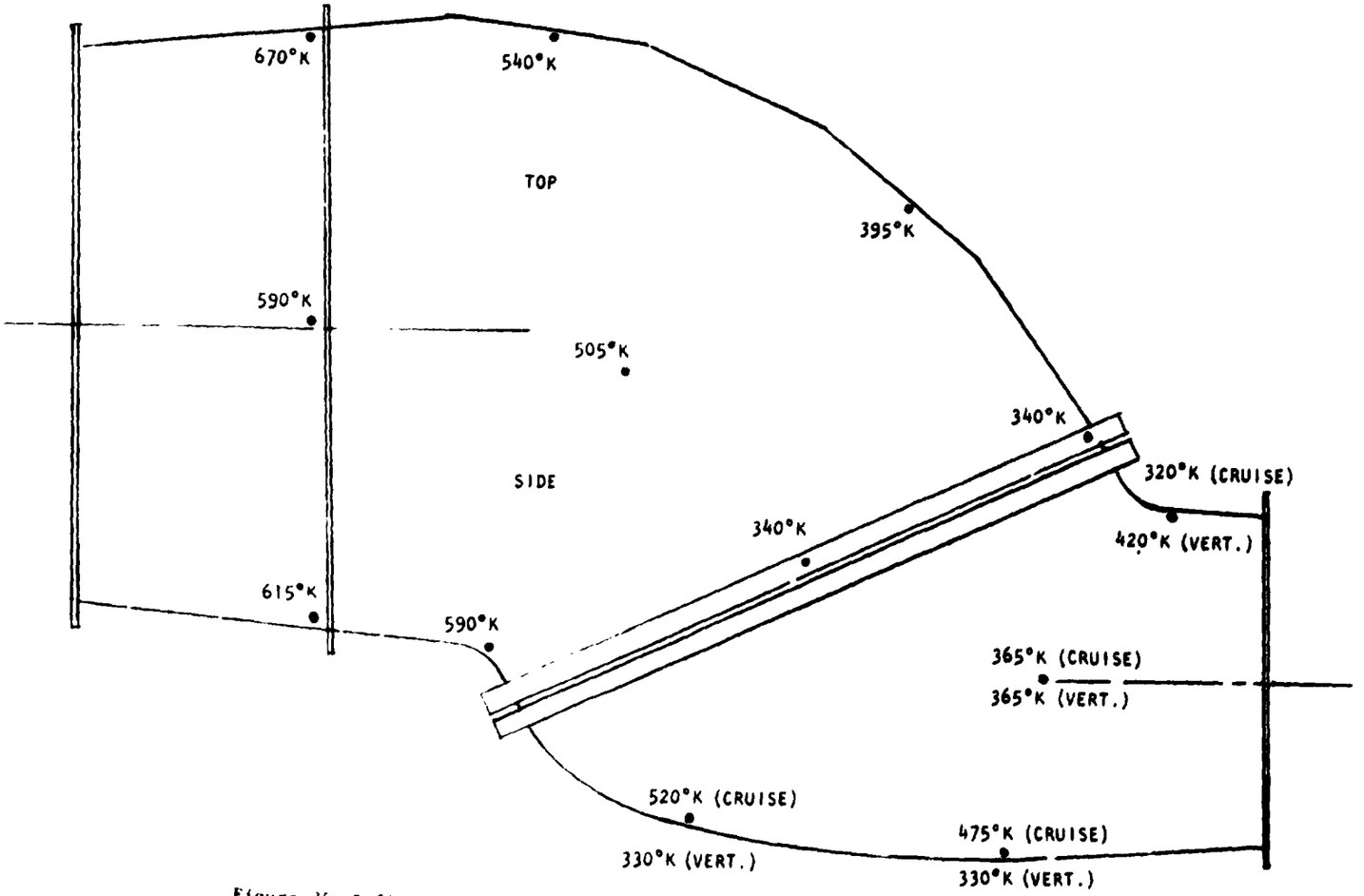

Figure 35. Deflector System Maximum Wall Temperatures During 90% Fan Speed Conditions

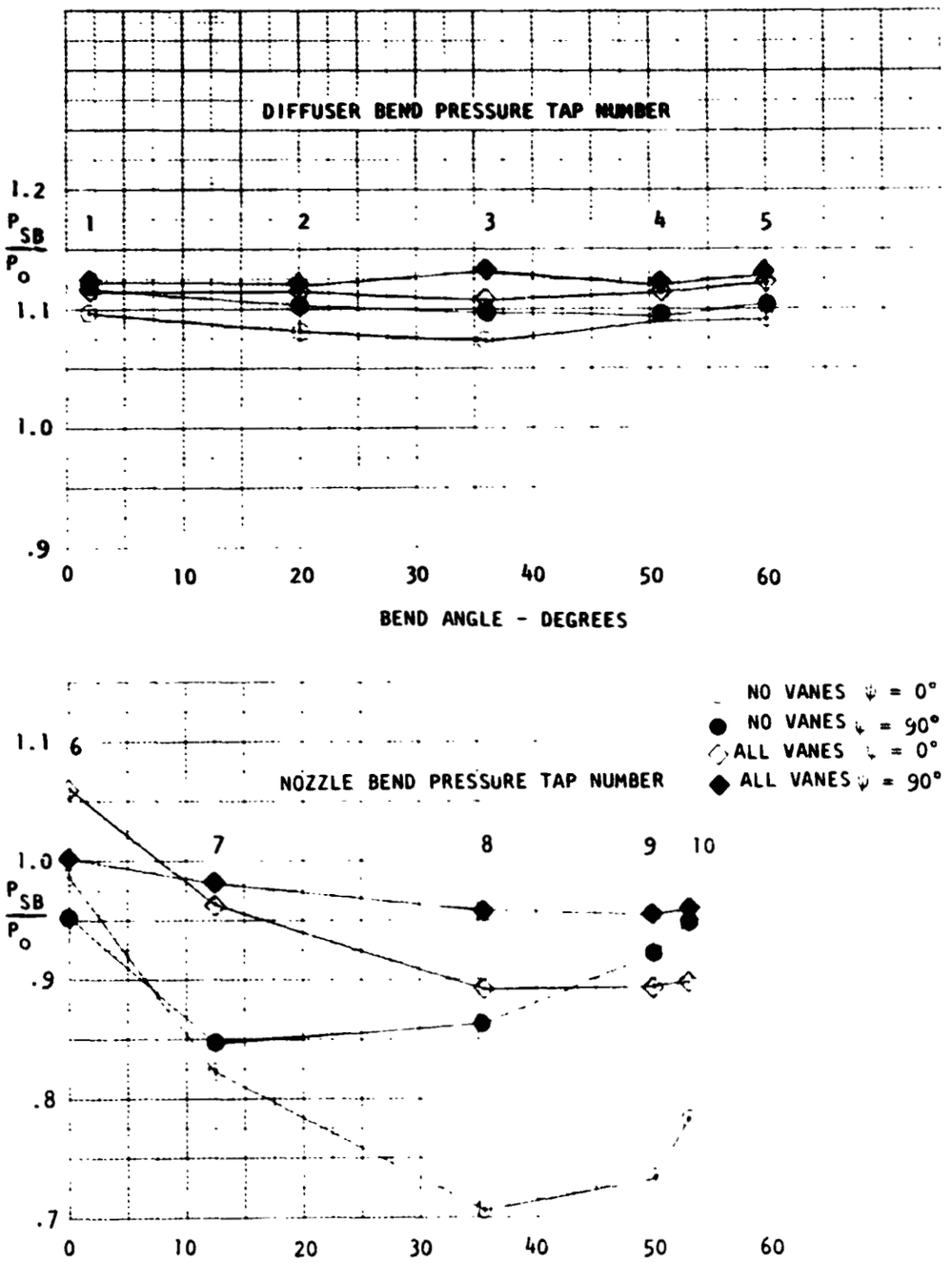

Figure 36. Static Pressure Ratio at Small Raduis Bends Vs. Bend Angle For 90% Fan Speed

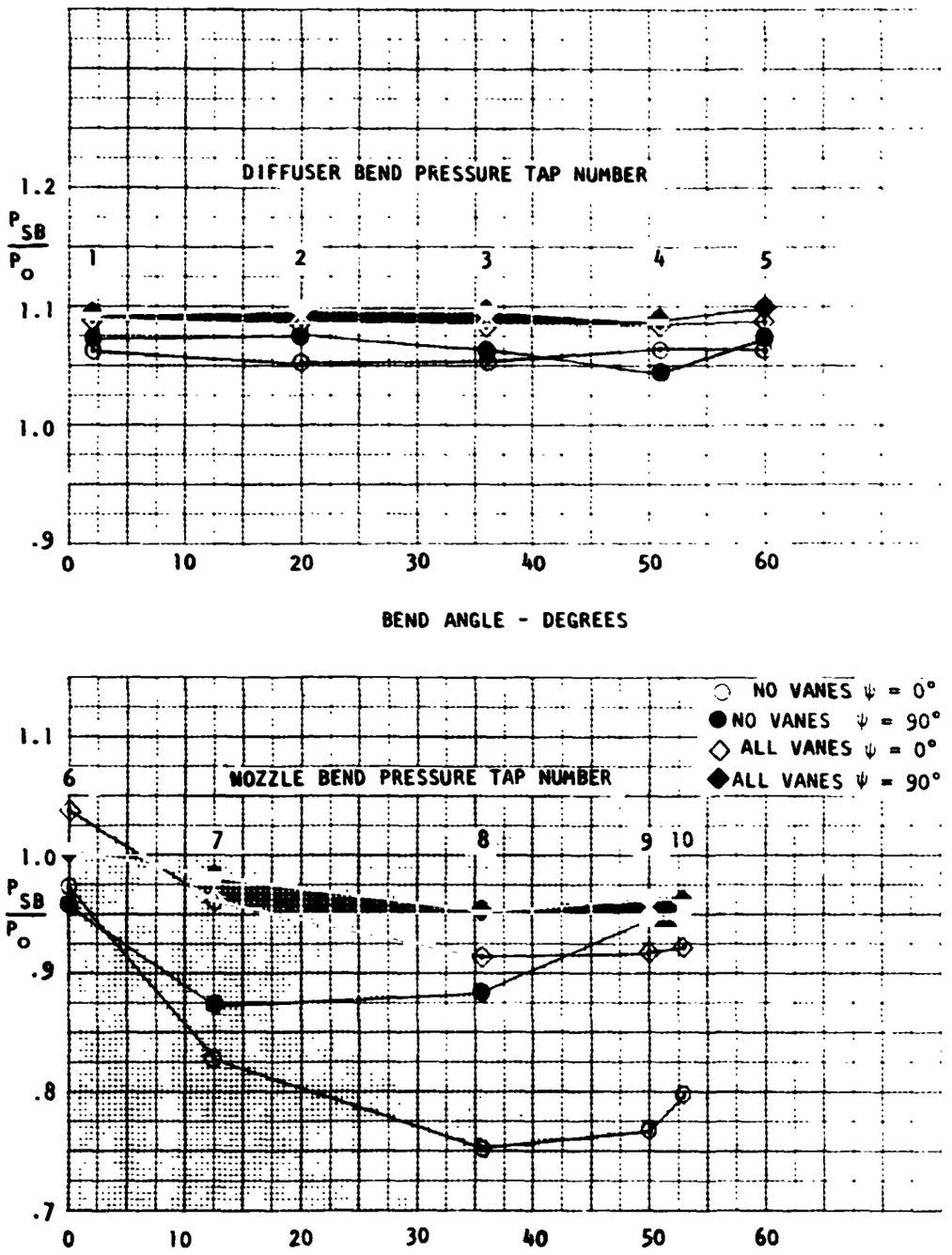

Figure 37. Static Pressure Ratio at Small Radius Bends Vs. Bend Angle For 80% Fan Speed

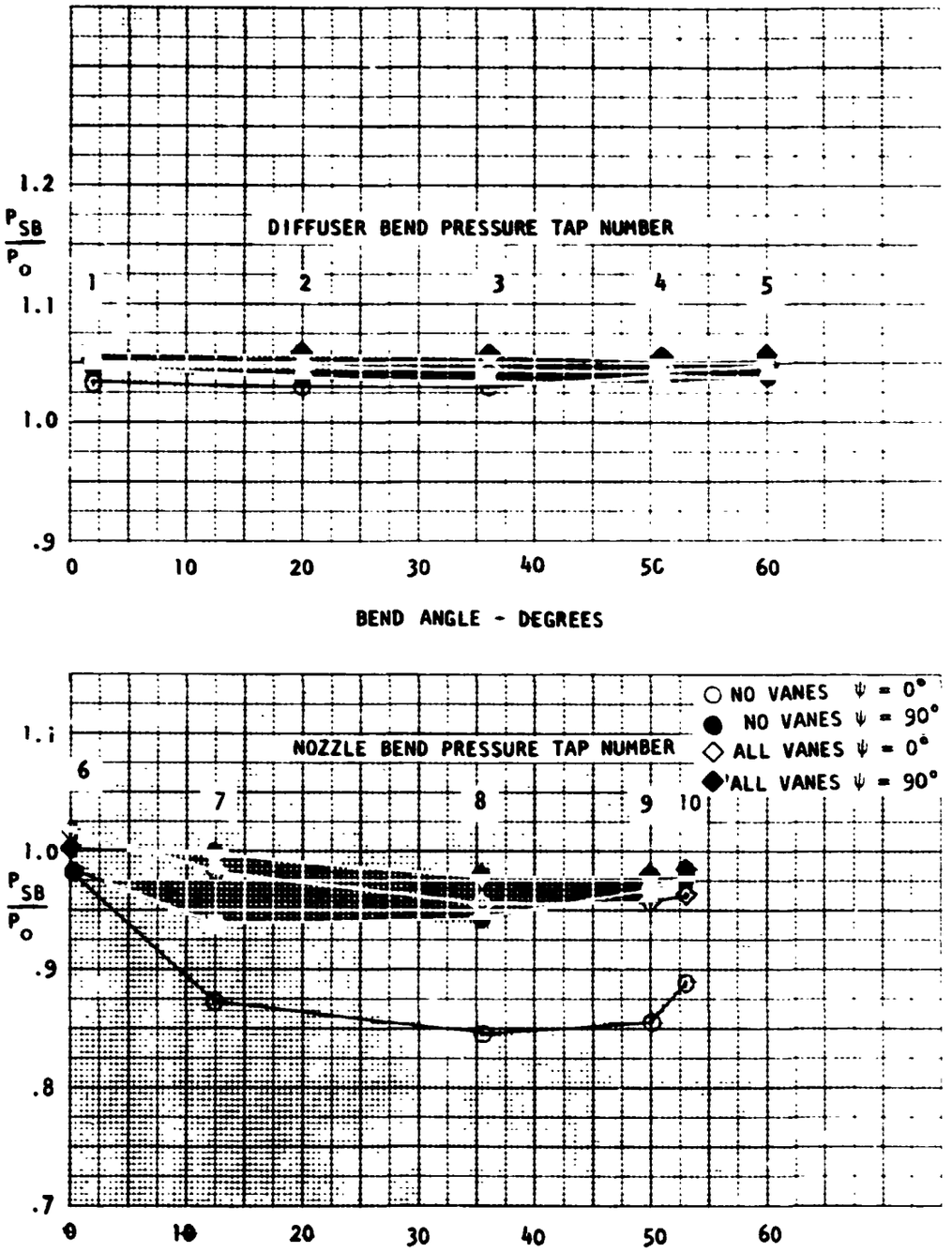

Figure 38. Static Pressure Ratio at Small Radius Bends Vs. Bend Angle For 60% Fan Speed

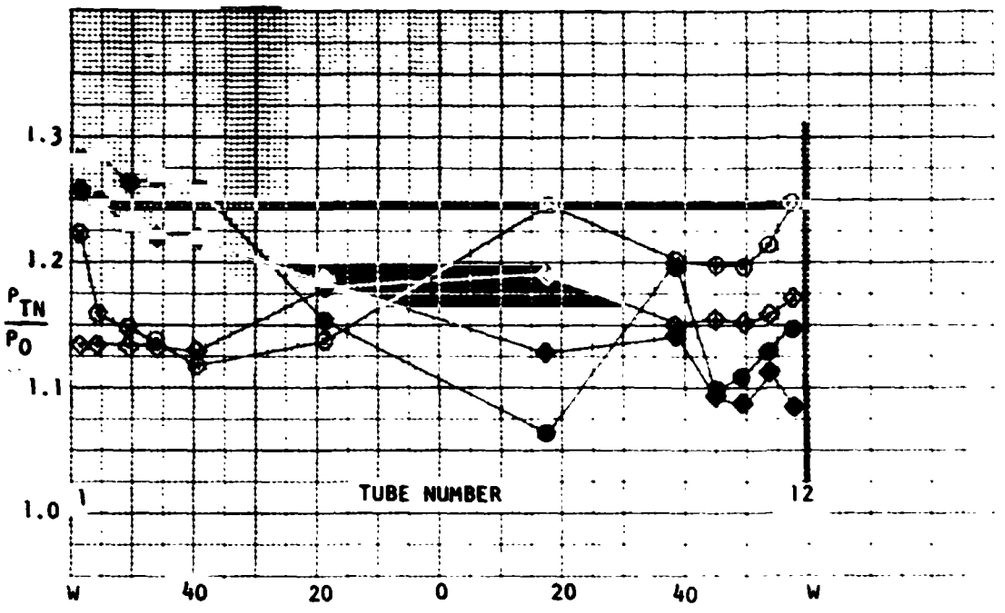

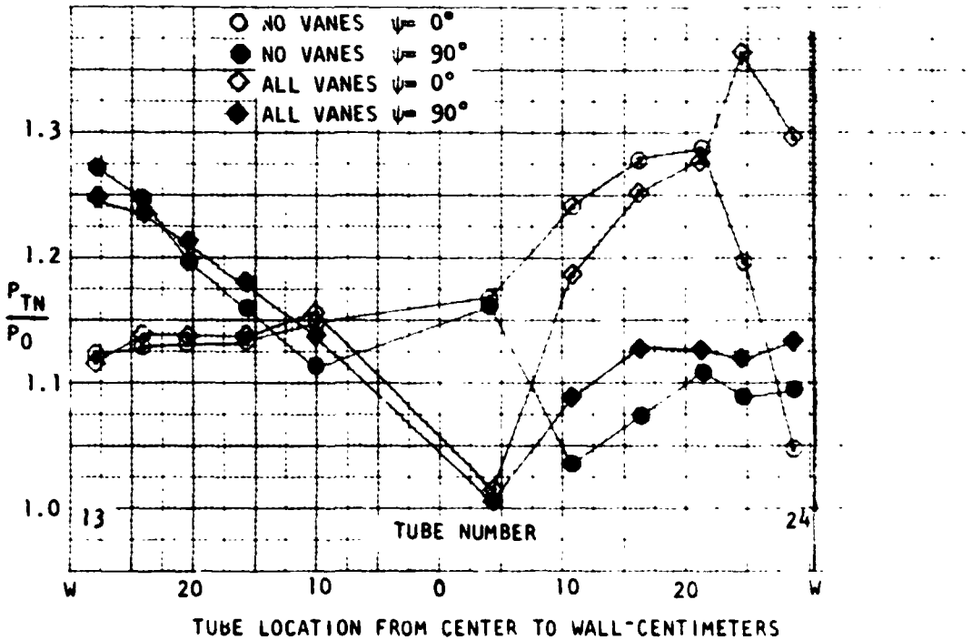

Figure 39. Exhaust Nozzle Total Pressure Ratio vs. Tube Location for 30% Fan Speed

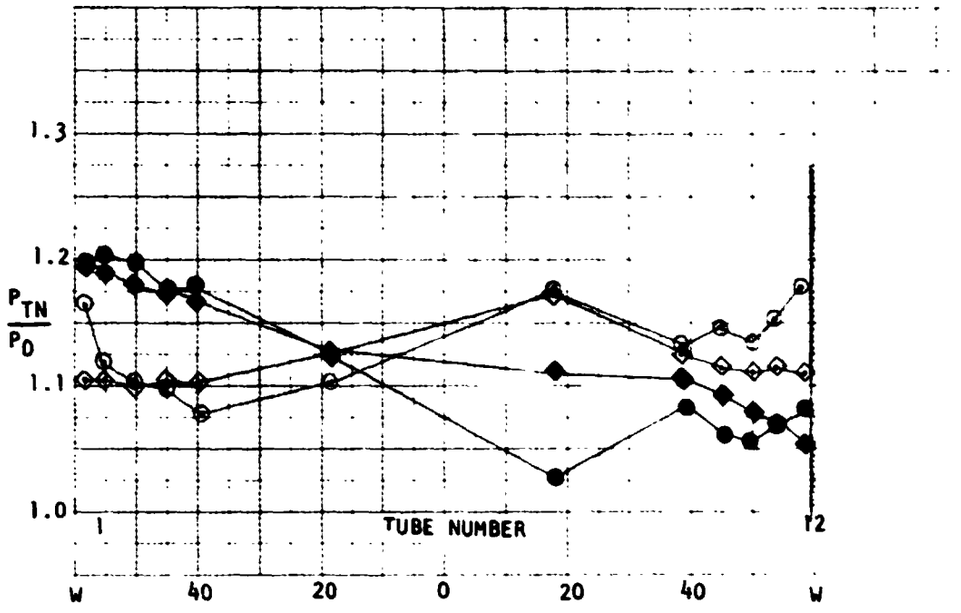

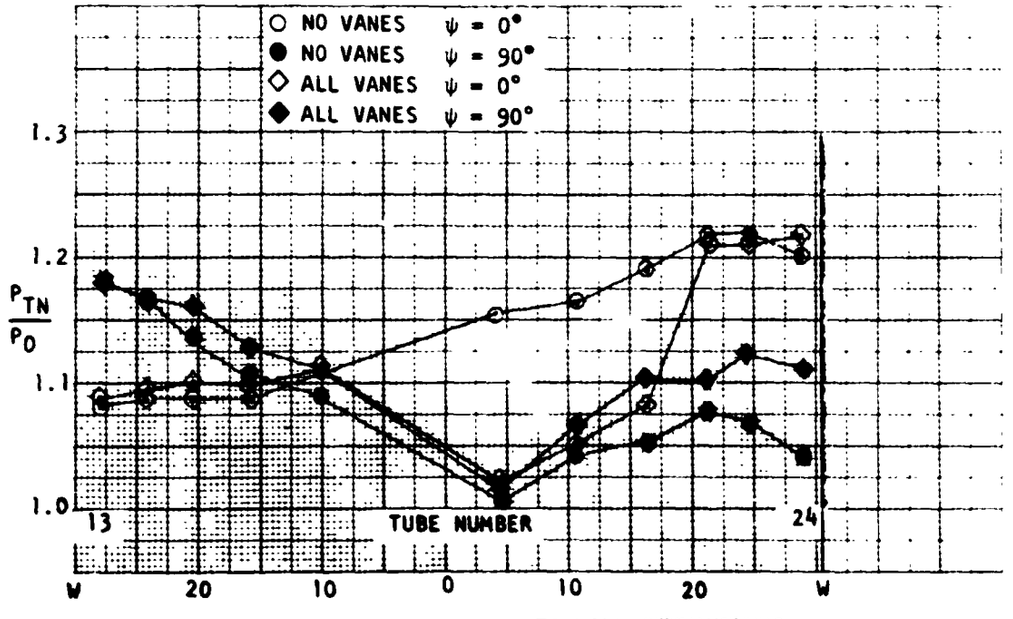

Figure 40. Exhaust Nozzle Total Pressure Ratio vs. Tube Location for 80% Fan Speed

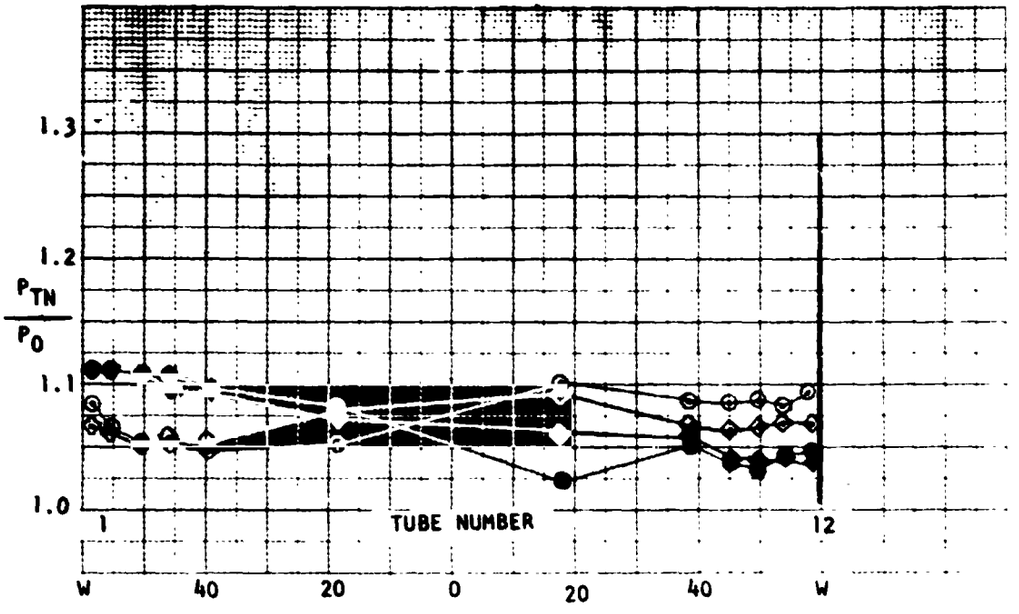

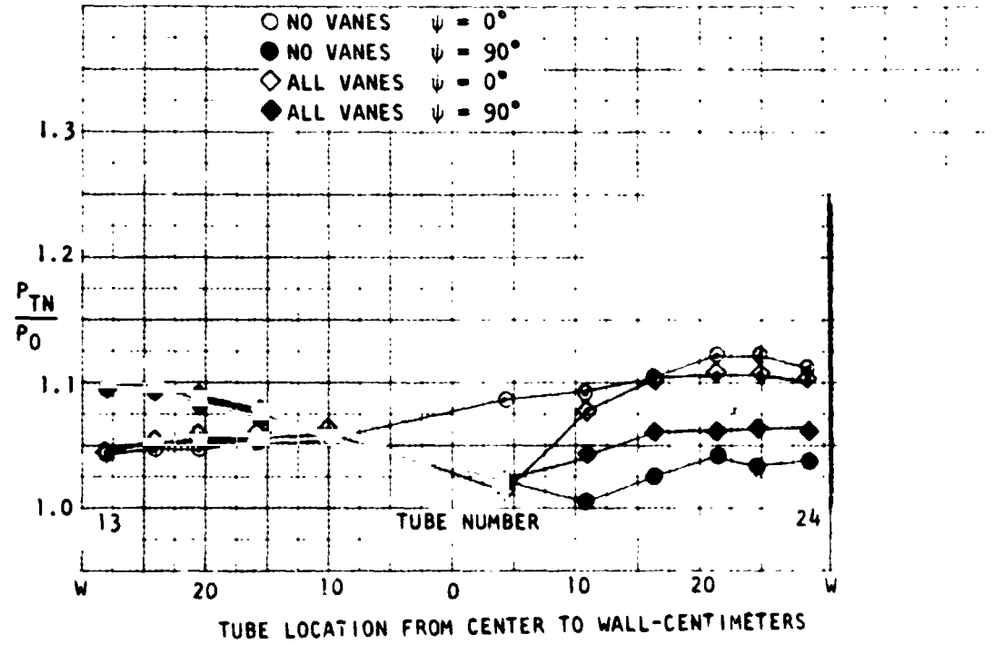

Figure 41. Exhaust Nozzle Total Pressure Ratio vs. Tube Location for 60% Fan Speed

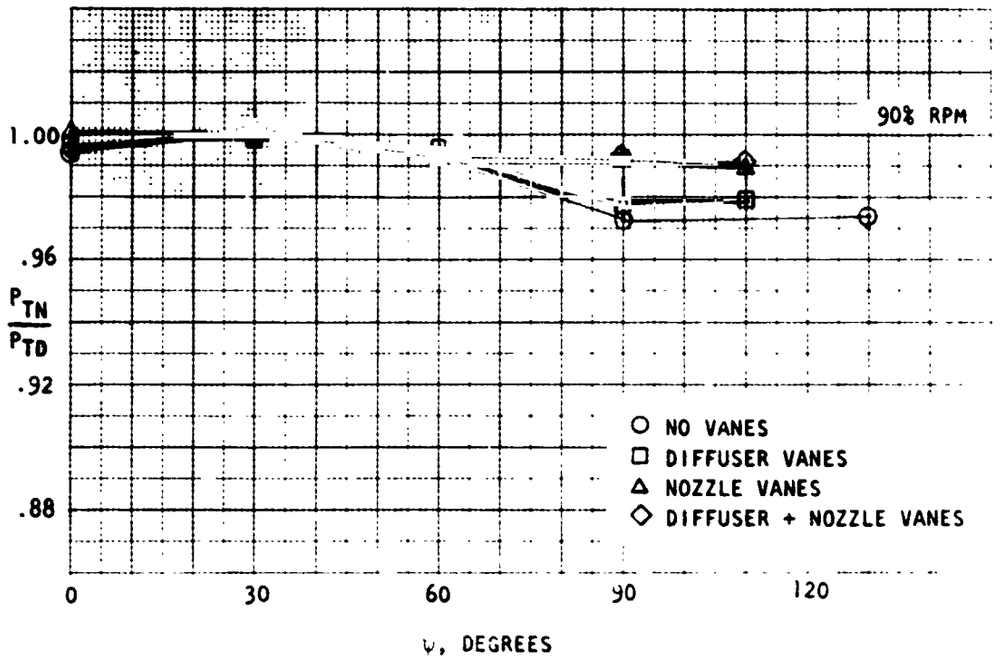

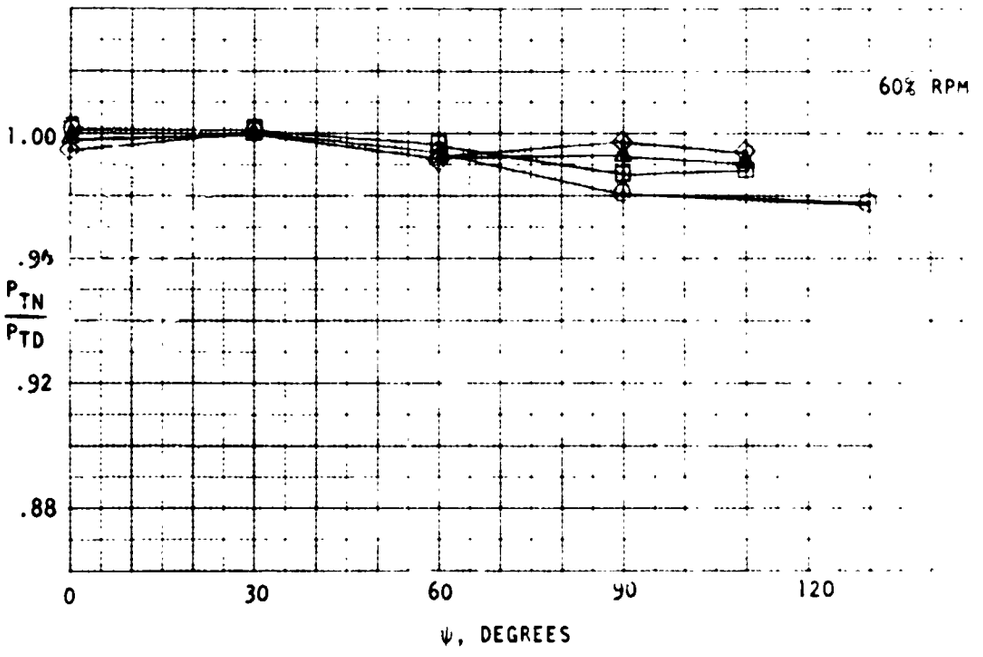

Figure 42. Exhaust Nozzle/Diffuser Exit Total Pressure Ratio Vs. Deflector Nozzle Angle For 90% and 60% Fan Speed

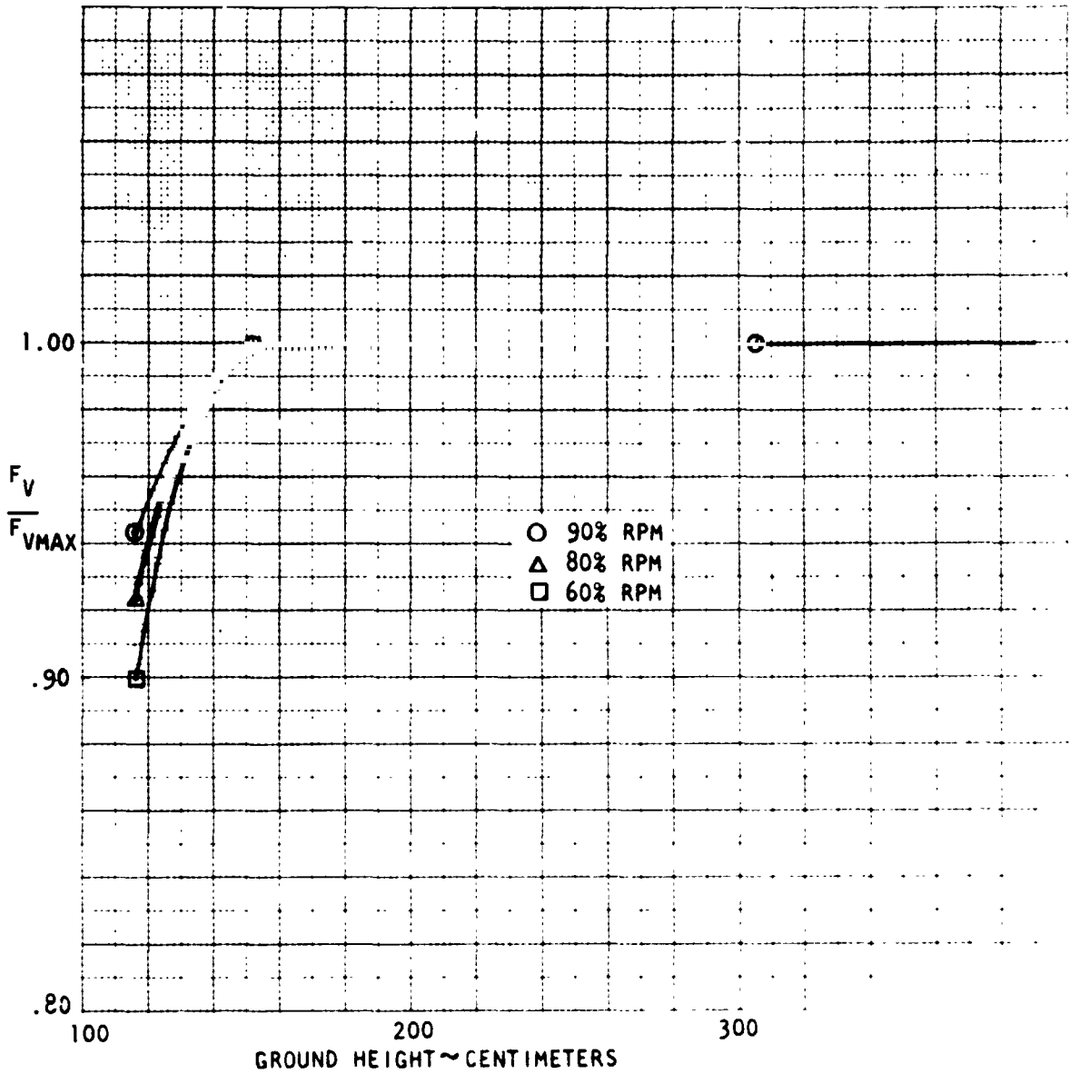

Figure 43. Effect of Ground Height To Nozzle Exhaust Plane On Vertical Thrust In 90° Deflection

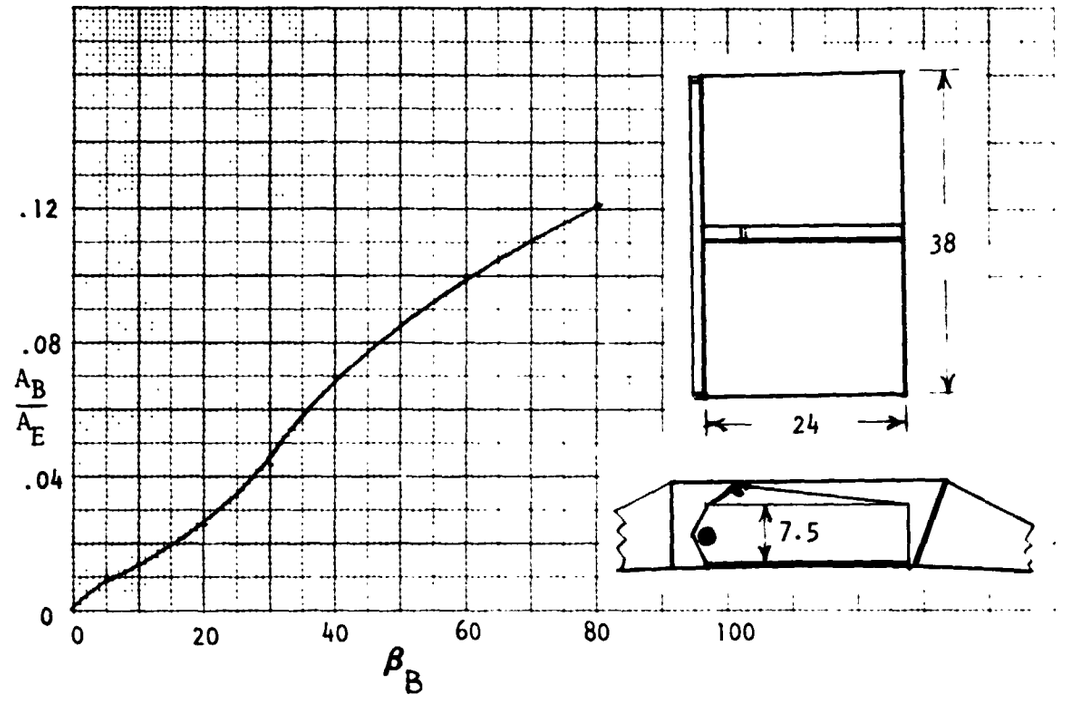

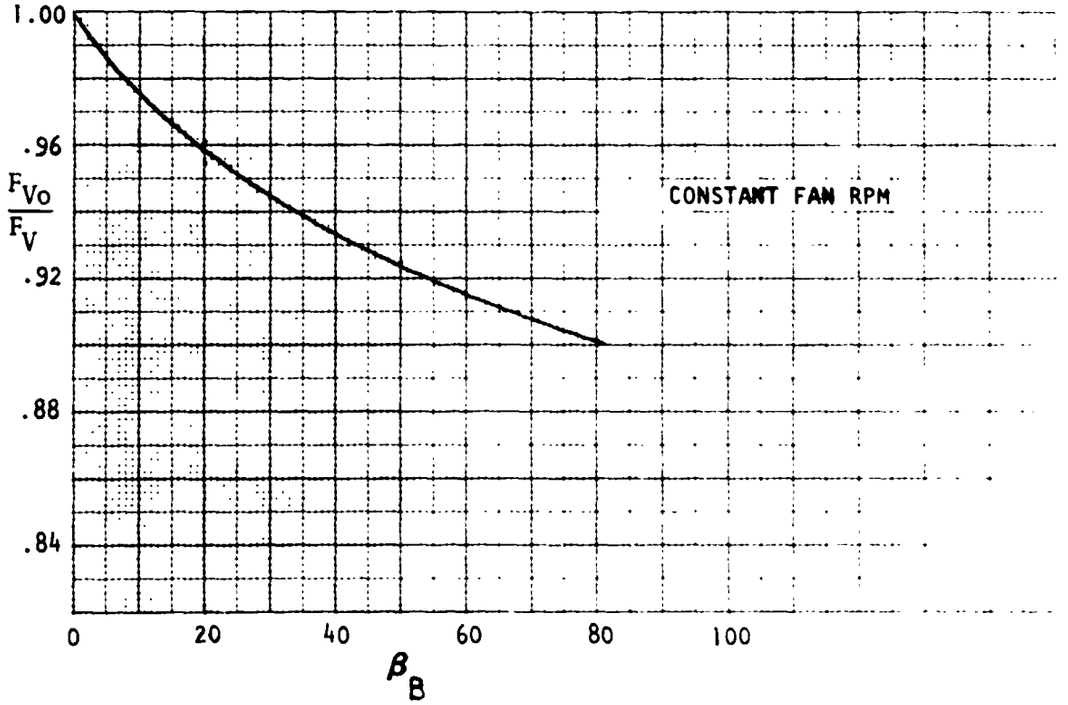

Figure 44. Diffuser Bypass Door Thrust Spoiling

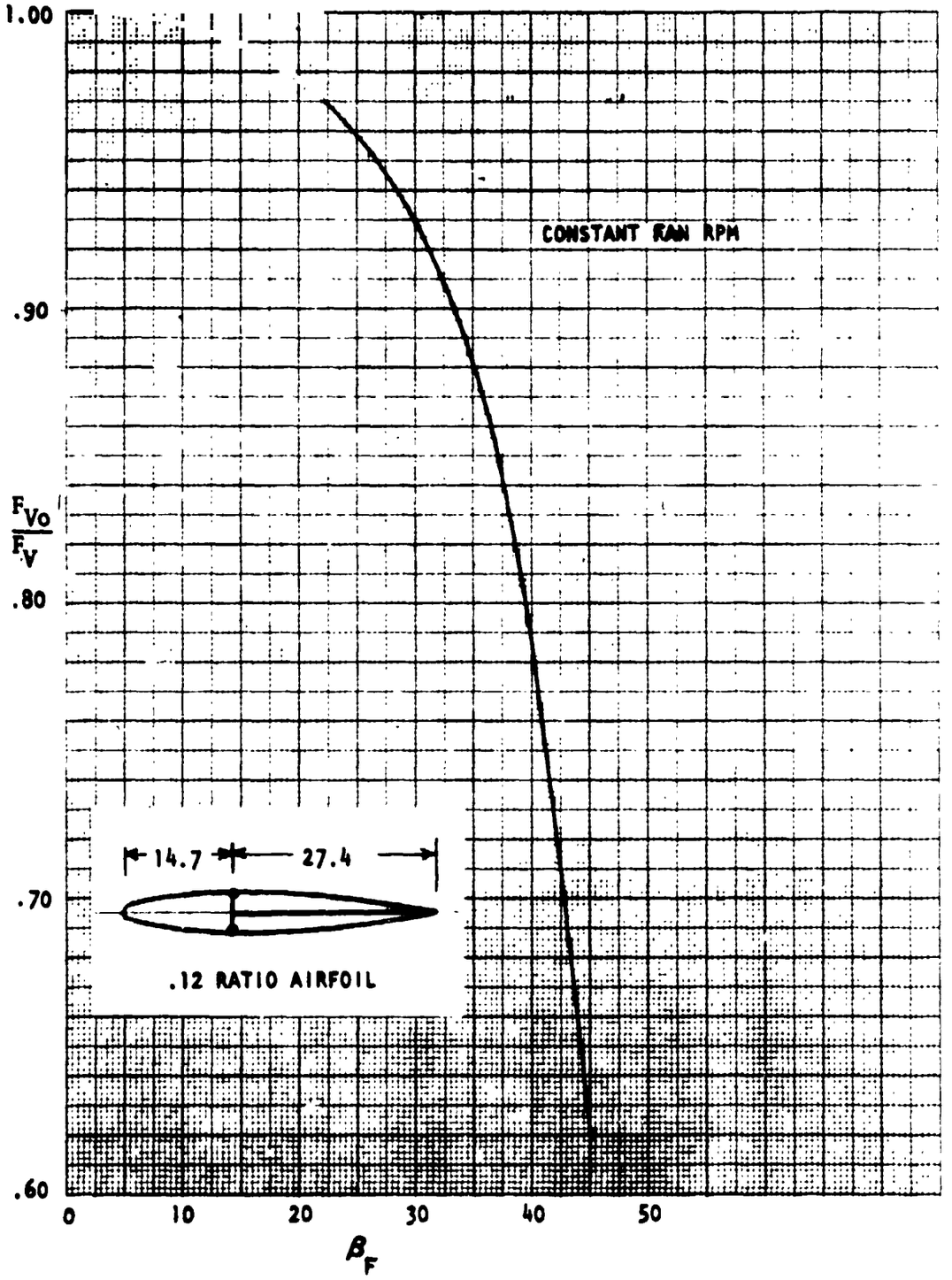

Figure 45. Nozzle Flap Thrust Spoiling